

1-1-2013

Encapsulation Through The Use Of Emulsified Microemulsions

Ruby R. Rafanan
ryerson

Follow this and additional works at: <http://digitalcommons.ryerson.ca/dissertations>

 Part of the [Molecular Biology Commons](#)

Recommended Citation

Rafanan, Ruby R., "Encapsulation Through The Use Of Emulsified Microemulsions" (2013). *Theses and dissertations*. Paper 2013.

This Thesis is brought to you for free and open access by Digital Commons @ Ryerson. It has been accepted for inclusion in Theses and dissertations by an authorized administrator of Digital Commons @ Ryerson. For more information, please contact bcameron@ryerson.ca.

ENCAPSULATION THROUGH THE USE OF EMULSIFIED MICROEMULSIONS

by

Ruby Rose Rafanan

B. Sc. (Applied Chemistry and Biology, Ryerson University)

A thesis

presented to Ryerson University

in partial fulfillment of the

requirements for the degree of

Master of Science

in the Program of

Molecular Science

Toronto, Ontario, Canada, 2013

©Ruby Rose Rafanan 2013

AUTHOR'S STATEMENT

I hereby declare that I am the sole author of this thesis. This is a true copy of the thesis, including any required final revisions, as accepted by my examiners.

I authorize Ryerson University to lend this thesis to other institutions or individuals for the purpose of scholarly research.

I further authorize Ryerson University to reproduce this thesis by photocopying or by other means, in total or in part, at the request of other institutions or individuals for the purpose of scholarly research.

I understand that my thesis may be made electronically available to the public.

ENCAPSULATION THROUGH THE USE OF EMULSIFIED MICROEMULSIONS

©Ruby Rose Rafanan

Master of Science, Molecular Science, Department of Chemistry and Biology
Ryerson University, Toronto, Ontario, Canada, 2013

ABSTRACT

Emulsified microemulsions (EMEs), first described in detail in 2005 by the group of Garti, consist of a thermodynamically stable water-in-oil microemulsion phase (w_1/o) further dispersed within an aqueous continuous phase (w_2). These internally-structured $w_1/o/w_2$ dispersions are promising controlled release vehicles for water-soluble flavouring compounds, drugs and nutraceuticals. With a stable internal droplet structure, storage stability is improved over non-thermodynamically stable structured emulsions and may exhibit unique controlled release behaviour. Use of food-grade components allows for wider and safer applications in food and pharmaceutical products. In this thesis, a food-grade w_1/o microemulsion consisting of glycerol monooleate, tricaprylin and water was dispersed in an aqueous (w_2) phase by membrane emulsification and stabilized by a caseinate-pectin complex to produce $w_1/o/w_2$ EMEs. The resulting EME showed no signs of phase separation for weeks at room temperature. The microemulsion and EME were characterized by differential scanning calorimetry (DSC), cryo-TEM and small angle x-ray scattering (SAXS) to determine whether the microemulsion's internal structure was maintained after emulsification. It was shown that EME droplets displayed ordering around the periphery consistent with some loss of microemulsion structure, but maintained the characteristic disordered microemulsion structure at the droplet core. Overall, this research demonstrated the feasibility of developing EME for possible applications in food and non-food applications.

ACKNOWLEDGEMENTS

Many people are to be acknowledged for their contribution to this work. Firstly, to the greatest lab group I have ever had the pleasure of working with. Its members, past and present, have made me a better researcher and realize the value of asking for help. A truly supportive and diverse group of people and I am fortunate have worked with you all. To my supervisory committee, D  rick Rousseau, Darrick Heyd and Daniel Foucher: thank you for your time, your guidance and encouragement throughout this entire journey. To Marcia Reid at McMaster University and Dr. Khursigura and Elyse Roach at University of Guelph, many thanks for providing your most excellent expertise in Cryo-TEM imaging. Your efforts are greatly appreciated. None of this work would be possible without generous funding from Ryerson University, Advanced Food and Materials Network (AFMnet) and Canadian Institute of Food Science and Technology (CIFST).

To my family, my mother and brother, and my friends, especially Tina Therrios, Garrett Jamieson, Aneesa Khan, Alexzander Samuelsson, Kate Melnychuk and Shaun Merritt: Thank you for seeing me through.

TABLE OF CONTENTS

<i>Title page</i>	i
<i>Author's Statement</i>	ii
<i>Abstract</i>	iii
<i>Acknowledgements</i>	iv
<i>Table of Contents</i>	v
<i>List of Tables</i>	vii
<i>List of Figures</i>	viii
<i>List of Appendices</i>	ix
<i>List of Abbreviations</i>	x
1. Introduction	1
1.1 Dispersed systems	2
1.1.1 Emulsions	2
1.1.2 Surface-active agents	4
1.2 Double emulsions	5
1.3 Microemulsions	6
1.3.1 Microemulsion formation	9
1.3.2 Characterization	10
1.3.3 Comparison to nanoemulsions	12
1.3.4 Applications of microemulsions	13
1.4 Emulsified microemulsions	14
1.4.1 Emulsified microemulsion formulations	17
1.4.2 Characterization	18
1.4.2.1 Small angle x-ray scattering (SAXS)	18
1.4.2.2 Cryo-TEM	19
1.5 Double emulsions in controlled release	20
1.6 Protein-polysaccharide emulsion stabilization	23
1.7 Research objectives	24
1.8 Hypotheses	25
2 Materials and methods	25
2.1 Materials	25

2.2	<i>Microemulsion formulation</i>	27
2.3	<i>Emulsified microemulsion formulation</i>	27
2.4	<i>Characterization</i>	29
2.4.1	<i>Droplet size distribution</i>	29
2.4.2	<i>Zeta potential</i>	29
2.4.4.	<i>Small angle x-ray scattering</i>	30
2.4.5.	<i>Differential scanning calorimetry</i>	31
2.4.6.	<i>Cryo-transmission electron microscopy</i>	31
2.4.7.	<i>Release behaviour</i>	32
2.4.8.	<i>Statistical Analysis</i>	32
	<i>Results and discussion</i>	33
2.5.	<i>Microemulsion formulation</i>	33
2.6.	<i>EME stability, droplet size distribution and zeta potential</i>	35
2.7.	<i>Differential scanning calorimetry</i>	38
2.8.	<i>Small angle x-ray scattering</i>	45
2.9.	<i>EME Cryo-TEM</i>	47
3.6.	<i>Release behaviour</i>	49
4.	<i>Conclusion</i>	52
4.1.	<i>Future Work</i>	54
5.	<i>Appendix</i>	55
6.	<i>Bibliography</i>	63

LIST OF TABLES

Table 1 - Constituent reagents and chemical structures used in this study to form food-grade EME.

Table 2 - Differential scanning calorimetry heating cycle enthalpic peaks for a 5% w/o microemulsion and bulk constituents.

Table 3 - Differential scanning calorimetry cooling cycle enthalpic peaks for a 5% w/o microemulsion and bulk constituents.

LIST OF FIGURES

Figure 1 - Surfactant volume distribution and effect on film curvature. Left: w/o, Right: o/w.

Figure 2 - Winsor classification of microemulsions (Winsor, 1948).

Figure 3 - Emulsified microemulsion domains as described by Yaghmur *et al.*, 2005.

Figure 4 - Schematic of membrane emulsification unit and mode of action. Left, lateral view of membrane emulsification unit. Right, oil droplets exiting pore outlets.

Figure 5 - Ternary phase diagram for the glycerol monooleate(GMO)-tricaprylin-water system at room temperature. The microemulsion region is shown along the GMO-tricaprylin axis. Dotted line corresponds to 5:5 dilution line used for formulating the microemulsions and EMEs used in this study.

Figure 6 - Cryo-TEM image of OsO₄-stained w/o microemulsion droplets.

Figure 7 - Light microscopy images of 1:3 casein-pectin stabilized dispersions on Day 0 at 630 X . Left: 15% w₁/o/w₂ EME, Right: 15% o/w emulsions. Bar = 20 μm.

Figure 8 - Droplet size distribution of 18% w/o/w EME and 20% o/w emulsion after 14 days of ageing at room temperature.

Figure 9 - Thermograms of a 5% w/o microemulsion and bulk constituents. Left: Heating, Right: Cooling.

Figure 10 - Thermograms of 20% EME and 20% o/w blank emulsion, Left: Heating, Right, Cooling.

Figure 11 - Small angle x-ray scattering diffractograms of 20% EME, 20% blank emulsion, non-dispersed microemulsion and 1:1 GMO:TC.

Figure 12 - Cryo-TEM of a dispersed oil droplet containing an inner microemulsion phase in partially vitrified ice, Left: Single oil droplet containing an EME. Right: Close magnification of EME droplet interface showing internal structure. Light areas within droplet correspond to microemulsion dispersed aqueous domains.

Figure 13- 48 hour release profiles of methylene blue in various matrices (EME, Emulsion, ME, aqueous phase).

LIST OF APPENDICES

Appendix 1 - Cooling thermogram of neat 1:1 GMO:TC.

Appendix 2 - Cooling thermogram of a 5% w/o microemulsion.

Appendix 3 - Cooling thermogram of neat GMO.

Appendix 4 - Cooling thermogram of neat TC.

Appendix 5 - Heating thermogram of 1:1 GMO:TC.

Appendix 6 - Heating thermogram of 5% w/o microemulsion.

Appendix 7 - Heating thermogram of neat GMO.

Appendix 8 - Heating thermogram of neat TC.

LIST OF ABBREVIATIONS

DE – Double emulsion

EME – Emulsified microemulsion

GMO – Glycerol monooleate

ME - Microemulsion

MB – Methylene blue

MBE – Methylene blue-loaded emulsion

MBEME – Methylene blue-loaded emulsified microemulsion

NaCas – Sodium caseinate

o/w – oil-in-water

TC – Tricaprylin

w/o – water-in-oil

1. INTRODUCTION

Controlled release and delivery of encapsulated compounds in food products and pharmaceuticals is an evolving and vital area of research that incorporates elements of material science, pharmaceutical science, food chemistry and biochemistry. This method of delivery is highly desirable for a number of reasons including improving dosing regimens, compound release under specific conditions, multiple compound packaging, and protection of target compounds (Gallarate, Carlotti, Trotta, & Ugazio, 2004; Garti, Yaghmur, Leser, Clement, & Watzke, 2001; Garti & Yuli-Amar, 2008; Spornath & Aserin, 2006).

One method of controlled delivery is to encapsulate the target compound within a dispersion, effectively trapping the compound of interest within a matrix. These particular systems are highly advantageous because they are customizable in many respects; however, they are limited in composition as products for human consumption must be made from only food or pharmaceutical-grade materials. These dispersions may be structured on the nanoscale level, exhibiting crystalline or disordered structure within dispersed droplets. Commonly-studied multiple emulsions may fall into this category, as well as emulsified liquid crystalline matrices and nanoemulsion-containing double emulsions. A nanostructured dispersion is of particular interest and has not been studied extensively.

The “emulsified microemulsion” (EME) is an emulsion whose droplets contain a thermodynamically-stable dispersion within them (Yaghmur, Campo, Sagalowicz, Leser, & Glatter, 2005; Yaghmur & Glatter, 2009). This system has the potential to be a highly efficient controlled release system which is resistant to degradation on account of the stable nanostructured droplets. Given the compositional limitations of food and pharmaceutical products, these EMEs have not been investigated extensively in terms of structure or function to prove their potential for encapsulation and controlled release applications.

This thesis aims to elucidate one such controlled release system composed entirely of food-grade materials in terms of its structure and functionality. A viable and novel food- and pharma - grade controlled delivery system was constructed, with its structure and encapsulation ability investigated. It was hypothesised that if a compound was encapsulated within a thermodynamically-stable, food-grade matrix and further dispersed within a continuous phase, a nanostructured emulsion (an EME), capable of retaining this compound more effectively than a non-nanostructured emulsion would result. As well, characterization methods determining structure of the system were applied to this food-grade EME.

1.1 DISPERSED SYSTEMS

Dispersions consist of one state of matter, referred to as the dispersed phase, distributed throughout a second, compositionally different medium, referred to as the continuous phase (Leal-Calderon, Bibette, & Schmitt, 2007; Rosen & Kunjappu, 2012). Both continuous and dispersed phases can occupy any of the three states of matter. Emulsions, microemulsions, solutions, aerosols and sols are common examples of dispersed systems, all of which have unique physical characteristics and behaviours (Dalgleish, 1996; Quemada & Langevin, 1985). Only structured emulsions and microemulsions will be further elucidated in this treatise.

1.1.1 EMULSIONS

Emulsions are common dispersions that consist of an insoluble phase dispersed within a solvent (Leal-Calderon *et al.*, 2007). In most cases, the phase that is the most abundant (on a weight or molar basis) is considered the continuous phase. Due to the incompatibility of the continuous and dispersed phases, a significant energy input is required to disperse one of the phases as droplets within the other phase. Turbulent force forms elongated areas of dispersed phase that

break into sections with further applied force eventually resulting in spherical droplets (Leal-Calderon *et al.*, 2007; Rosen & Kunjappu, 2012). Organic phases, either polar or non-polar, are often referred to as “oil” when referring to food-related systems. This convention will be followed for the remainder of this work. Emulsions can be of two main types: oil droplets dispersed in a continuous water phase (oil-in-water, o/w), or water droplets dispersed in oil (water-in-oil, w/o). These emulsions are used in various products, from food to pharmaceuticals. Common w/o emulsions encountered as food products include butter and margarines, while milk/cream and mayonnaise are of the o/w emulsion type (Dalglish, 1996).

Since the system experiences a high interfacial tension between the two phases and strong shearing forces are necessary to form these emulsions, an emulsion is inherently thermodynamically-unstable and prone to separation into their respective bulk phases (Rosen & Kunjappu, 2012). In order to overcome eventual coalescence and phase separation, the use of surface-active agents is commonly employed. Surfactants are amphiphilic compounds that interact at the interface between the two phases (*i.e.*, at the droplet surface of the dispersed phase). This interaction reduces the interfacial tension, rendering the dispersed phase more ‘soluble’ and the interface more pliable (Quemada & Langevin, 1985; Rosen & Kunjappu, 2012). In aqueous systems, the surfactant is ideally present as a monolayer and in equilibrium with excess surfactant in the continuous phase (Langevin, 1992). In o/w emulsions, the interfacial tension between the continuous aqueous phase and the monolayer at the oil droplet surface is related by Equation 1

$$\gamma = \gamma_w \pi \quad (1)$$

where γ is interfacial tension, γ_w is the water surface tension and π is the surface pressure at the oil-water interface (Langevin, 1988).

1.1.2 SURFACE-ACTIVE AGENTS

Surface-active agents (also known as surfactants or emulsifiers), are varied in their molecular structure, but all are amphiphilic, consisting of polar and non-polar regions. Surfactants may be ionic, non-ionic or zwitterionic. Ionic surfactants may be cationic (*i.e.* quaternary ammonium salts) or anionic (*i.e.* sodium dodecyl sulfate). These particular types of surfactants are suitable as a dispersant or lathering agent, but are not suitable for food and pharmaceutical purposes due to their toxicity. Zwitterionic surfactants, such as imidazoline carboxylates, contain areas of both positive and negative charge. These types of surfactants are often found in industrial detergents and cosmetics. Nonionic surfactants are neutral molecules with no charged regions. Polysorbates and monoglycerides fall under this category and many are used in food products due to their low toxicity (Rosen & Kunjappu, 2012). At the interface between two immiscible fluids, the polar end of the surfactant molecule interacts with the polar phase while the non-polar end interacts with the oil phase (Rosen & Kunjappu, 2012).

The efficiency of a surface-active agent to stabilize a particular dispersion is determined by its HLB, or hydrophilic-lipophilic balance value (Constantinides & Scalart, 1997). This is a numerical scale, typically from 1-20, where surfactants displaying a low HLB value tend to stabilize w/o dispersions whereas a higher-valued surfactant will tend to form o/w dispersions. The well-known Bancroft Rule stipulates that the surfactant film will bend towards the phase in which the surfactant is most soluble (Langevin, 1992; Rosen & Kunjappu, 2012). The preferential bending of the film, C_0 , may be towards either phase and is largely dependent on the volume occupied by the polar and non-polar regions of the surfactant molecule. A large polar region in comparison to the non-polar region will stabilize oil droplets in water, bending the film towards the water phase. By convention, C_0 is a positive integer. Likewise, a large non-polar volume in comparison to the polar region will cause film deformation towards the oil continuous phase and will have a negative C_0 .

value (Langevin, 1988, 1992). The relationship between film curvature, surfactant region volume distribution and droplet identity is depicted in Figure 1.

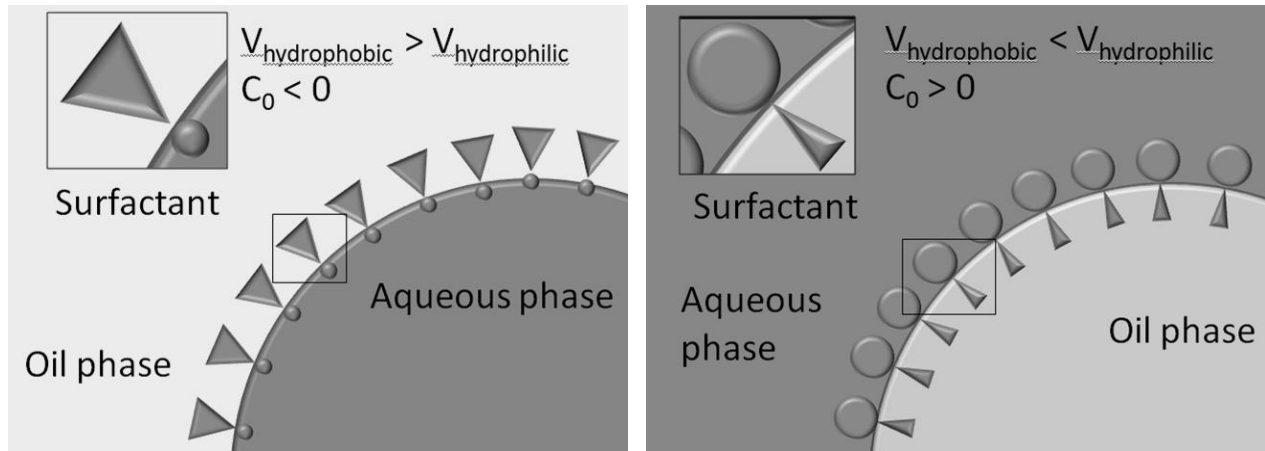


Figure 1 - Surfactant volume distribution and effect on film curvature. Left: w/o, Right: o/w.

1.2 DOUBLE EMULSIONS

Double emulsions (DEs) encompass two categories: i) water-in-oil-in-water ($w_1/o/w_2$) emulsions, where water droplets are dispersed in oil droplets, which in turn are dispersed in a continuous aqueous phase, and ii) oil-in-water-in-oil systems where oil droplets are located within water droplets that are dispersed within a continuous oil ($o_1/w/o_2$). Though the former is more frequently studied, applications using either DE type have been developed for food, pharmaceutical and cosmetics use (Dickinson, 2010a; Ficheux, Bonakdar, & Bibette, 1998; Garti & Benichou, 2004; Kanouni, Rosano, & Naouli, 2002; Morais, Santos, Nunes, Zanatta, & Rocha-Filho, 2008).

DEs are typically more difficult to prepare and control than simple emulsions, in large part given the presence of two thermodynamically-unstable interfaces (Garti & Benichou, 2004). Generally, the construction of a stable multiple emulsion requires the use of two or more surfactants. As well, these structured emulsions often require a multi-step process to be generated. Typically, a coarse emulsion is made first which comprises the internal emulsion. In the case of

$w_1/o/w_2$ DEs, a w_1/o emulsion is formed first which is then dispersed in an aqueous continuous phase. The reverse compositions will yield an $o_1/w/o_2$ DE. The internal emulsion requires the formation of very fine droplets, and usually involves the use of high energy dispersion methods. The internal emulsion can be dispersed in a variety of ways, including high pressure homogenization, membrane emulsification and shearing (Benichou, Aserin, & Garti, 2007a, 2007b; Higashi, Shimizu, Uchiyama, Tamura, & Setoguchi, 1995; Joscelyne & Trägårdh, 2000).

The use of multiple surfactants is essential in maintaining DE integrity. Usually, the mix of surfactant consists of low and high HLB surfactants (Ficheux *et al.*, 1998; Garti & Benichou, 2004; Kanouni *et al.*, 2002). In the case of a $w_1/o/w_2$, the primary emulsion contains a low HLB surfactant to form fine water droplets in oil. This is then emulsified into the w_2 phase containing a high HLB surfactant which stabilizes the overall emulsion (Benichou *et al.*, 2007b). Primary emulsions in $o_1/w/o_2$ DEs contain a high HLB surfactant. This is stabilized in the w_2 phase using a low HLB surfactant (Benichou *et al.*, 2007b).

These particular dispersions are not thermodynamically stable and will eventually lose the inner structure due to various processes, namely coalescence and/or Ostwald ripening (Garti & Benichou, 2004). If used as an encapsulation matrix, in losing its inner emulsion, a compound of interest within the inner phase of the DE may be uncontrollably released into the continuous phase. Hence, DE instability and unpredictability in release kinetics pose a significant problem that may be remedied by increasing the stability of the internal droplets. This instability and its relation to release of encapsulated compounds will be discussed in a proceeding section.

1.3 MICROEMULSIONS

Microemulsions are spontaneously-forming, thermodynamically-stable dispersions that behave as Newtonian fluids (Friberg, 1985; Quemada & Langevin, 1985). The dispersed phase is most often in droplet (spherical) form, however, cylindrical and ovoid shapes have been reported

(Ezrahi, Tuval, & Aserin, 2006; Langevin, 1992; Lawrence & Rees, 2000). Classical, spherical microemulsion droplet sizes are normally well-below 100 nm in diameter (Rakshit & Moulik, 2009). Small droplet size and spontaneous formation are achieved due to a high concentration of surfactant and often by the presence of a co-surfactant, which is a small molecule that is not surface-active, but alters the film curvature by increasing the flexibility of packed interfacial films (Quemada & Langevin, 1985). The co-surfactant is usually located near the interface (often interspersed amongst surfactant molecules) and may be soluble in either the dispersed or continuous phase (Rosen & Kunjappu, 2012). The surfactant's head group area, length and volume will influence its critical packing parameter (CPP), which ultimately determines droplet size and identity. Short-chained triglyceride oils and alcohols can affect the CPP of a given surfactant by increasing the hydrophobic tail volume (Langevin, 1992). These additives fill voids between surfactant molecules and influence the curve (C_0) of the film by increasing or decreasing the curve towards or away from the droplet (Quemada & Langevin, 1985). Co-surfactants are not compulsory for microemulsion formation (Constantinides & Scalart, 1997; Quemada & Langevin, 1985), but do influence droplet size owing to the change in CPP (Zhang *et al.*, 2008), Winsor classification and shape (Quemada & Langevin, 1985).

Microemulsions can exist in one of four forms (Figure 2). The naming convention follows those characterized by Winsor (Winsor, 1948). Winsor I and II microemulsions are two-phase mixtures consisting of a microemulsion phase co-existing with excess dispersed phase. Winsor I (S1) is an o/w microemulsion in equilibrium with excess oil. Winsor II (S2) is a w/o microemulsion in equilibrium with excess water. The microemulsions in each of these systems are thought to be saturated with dispersed phase, causing the excess dispersed phase to accumulate separately from the dispersion, forming a distinct secondary layer. Winsor III microemulsions (S3) can be a two- or three-phase system where a bicontinuous microemulsion is formed with excess phases, either water or oil. The bicontinuous structure is not an ordered assembly of parallel and evenly spaced

water and oil regions as is seen with a lamellar structure, but rather resembles a random arrangement of elongated “stacks” of water and oil compartments (Figure 2) (Winsor, 1948). A Winsor IV structure (S4) is a surfactant-rich, isotropic dispersion consisting of either a w/o or o/w ME.

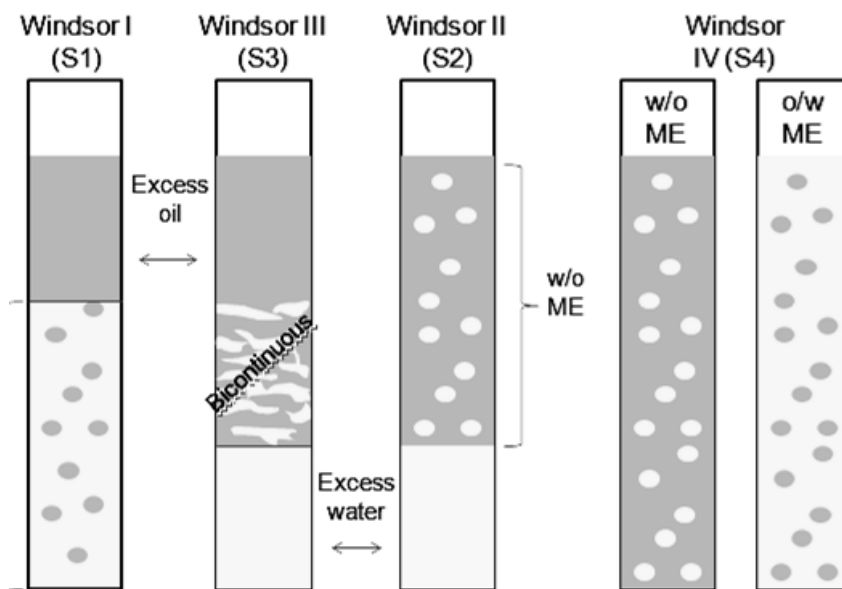


Figure 2 - Winsor classification of microemulsions (Adpated from Winsor, 1948).

Microemulsions are highly sensitive to component ratios and temperature. Changes in the surfactant, oil or water content may elicit a change in the structure of the system (Kunieda & Shinoda, 1985; Langevin, 1992; Rakshit & Moulik, 2009) by inverting to a w/o to o/w dispersion or *vice versa*. Temperature is also a key parameter when characterizing a microemulsion. Phase inversion may occur due to a change in solubility in surfactants where the surfactant(s) may exhibit varying solubility with varying temperature (Shinoda & Saito, 1968).

1.3.1 MICROEMULSION FORMATION

Originally, when attempting to explain microemulsion formation, it was thought that the system experienced a transiently negative interfacial tension. However, this has been thought to be an oversimplification as other factors have a far greater influence on interfacial film phenomena.

The free energy change on mixing (ΔG_{mixing}) may be calculated using Equation (2):

$$\Delta G_{\text{mixing}} = \Delta G_1 + \Delta G_2 - T\Delta S_{\text{mixing}} \quad (2)$$

where ΔG_1 is dependent on the change in surface tension and the formation of an electrical double layer. The electrical double layer is the formation of two layers of opposing charge, one at the interface and the other of counterions surrounding the primary layer. ΔG_2 depends on the interaction between adjacent droplets. The electrostatic stabilization provided by the double layer provides the prevalent force required to prevent coalescence between droplets. These two ΔG values provide the conditions under which a microemulsion can form, but do not necessarily provide a negative ΔG_{mixing} value. The most influential factor determining microemulsion formation is the entropic contribution, $T\Delta S$, where T and S are temperature and entropy, respectively. The formation of many small droplets (less than 100 nm) increases the entropy of the system by providing many possible configurations to the system (*e.g.*, droplet locations in a given volume). When droplet size is sufficiently low and the number of droplets formed is sufficiently high, the entropic term is large enough overcome ΔG_1 and ΔG_2 to provide a negative ΔG_{mixing} value. Under these conditions, formation is considered spontaneous (Ruckenstein & Chi, 1974).

An ultra-low interfacial tension, on the order of 10^{-2} mN/m, is necessary to keep ΔG values below zero (Langevin, 1992). This allows for thermodynamic conditions allowing for self-assembly and is usually provided by high surfactant concentrations, equivalent or greater than the critical micelle concentration (Lawrence & Rees, 2000). Presence of a surfactant at the interface of oil and water renders the film more pliable by making the film more disordered and entropically more favourable. This disorder is enhanced by mixing. With gentle agitation, the surfactant monolayer

bends the film in the direction that satisfies the surfactant volume distribution (*i.e.*, $C_0 < 0$, w/o; $C_0 > 0$, o/w). The result is an aggregate of surfactants, similar to surfactant aggregation in solution. This type of dispersion is often thought of as swollen micelles (McClements, 2012) as these systems are not merely surfactant aggregates in a continuous phase, but contain a distinct dispersed phase within the core of the micelle.

1.3.2 CHARACTERIZATION

As mentioned, an ultralow interfacial tension is characteristic of microemulsions owing to the high concentration of surfactants. Tensions of $< 10^{-2}$ mN/m are often measured by spinning drop tensiometers (Langevin, 1988). This method involves measuring the deformation of a droplet suspended in a solvent of greater density under centripetal force.

A characteristic of w/o microemulsions is the presence of a water “core” within the aqueous droplets (or domains). There is a definite free water region within each microemulsion droplet distinct from interfacial water which interacts with the hydrophilic moiety of the surfactant (Ezrahi *et al.*, 2002; Ezrahi, Aserin, Fanun, & Garti, 2000; Garti, Aserin, Tiunova, & Fanun, 2000; Schulz, 1998; Senatra, 2000). These unique species of water within each droplet may be discerned through the use of numerous techniques including differential scanning calorimetry (DSC). Free water (*i.e.*, bulk water), when present within a w/o microemulsion, will have melting and freezing points similar to that of pure water. Interfacial water will freeze and melt at lower and higher temperatures, respectively (Ezrahi *et al.*, 2000; Senatra, 2000). As a result, DSC may be used to distinguish the different ‘types’ of water based on this property.

Bound water is structurally distinct from bulk (free) water. This form of water creates a layer about the interface of a microemulsion droplet, creating what is referred to as a hydration shell. When present at the interface, water will solvate the polar region of the surfactant, the extent of which is dependent on the number and type of functional groups present (Schulz, 1998). The

thickness of this layer has been estimated to be anywhere between 0.3 nm to 10 nm for various surfactants, indicating that this is a highly variable region that is largely dependent on surfactant type and how the polar moiety is able to structure water near the interface (Garti *et al.*, 2000; Schulz, 1998). DSC studies examining interfacial water have examined water-water hydrogen bonding as well as surfactant-water hydrogen bonding. Elucidating interfacial water structure is a delicate task as various surfactants are able to “structure” water more strongly than others, such as charged phenyl or butyl groups (Schulz, 1998). In general, charged headgroups will yield more structured water whereas non-ionic surfactants with large polyoxyethylene groups do not structure water effectively and yield less structured water within the hydration layer than bulk (free) water.

As well, DSC can be used to determine how various components interact with each other after microemulsion formation (Narang, Delmarre, & Gao, 2007). DSC can be used as a tool to determine whether a dispersion is simply a micellar solution where surfactant aggregates are simply hydrated or rather resembles a true microemulsion (specifically w/o) with a water core in addition to water interacting with the surfactant (Senatra, 2000).

When characterizing a w/o microemulsion with this method, the thermal signature of an initially water-poor sample will be compared to that of samples containing increasing amounts of water. An enthalpic peak will evolve corresponding to the interfacial water in the system. As water concentration increases, this peak will eventually cease to grow when the interface is maximally hydrated. However, a peak corresponding to free water in the system will continue to increase with increasing water content (Garti *et al.*, 2000). Interfacial water has a characteristically low liquid-solid transition temperature which is dependent on surfactant identity (Schulz, 1998), presence of a co-surfactant (Ezrahi *et al.*, 2002) and HLB value (Garti *et al.*, 2000).

There are instances in the scientific literature regarding the novel use of free vs. bound water as a reaction tool. For example, the presence of these two forms of water in microemulsions has been applied for use in synthetic reactions where microemulsions behave as a dispersant.

Libster *et al.* solubilized a nucleating agent in a w/o microemulsion and introduced it into a polypropylene suspension (Libster, Aserin, & Garti, 2006). Presence of a microemulsion-based nucleator improved polypropylene crystallization, yielding superior optical and mechanical properties to a conventionally-produced control. Microemulsion phase transitions monitored by DSC showed that the free water content within the microemulsion was correlated to improved nucleator loading and its subsequent dispersion during polypropylene crystallization. Based on this and other studies, DSC is a reliable method to optimize surfactant choice to tailor microenvironments used in microemulsion catalysis and dispersion vehicles, making it especially useful in the development of new products.

1.3.3 COMPARISON TO NANOEMULSIONS

Nanoemulsions, contrary to what the name suggests, are not synonymous with microemulsions. Although the size domains of both systems are quite small, the differentiating factor between the two is that nanoemulsions are not thermodynamically-stable whereas microemulsions are (McClements, 2012). Nanoemulsions are often manufactured with a far lower surfactant concentration than microemulsions and usually require high energy dispersion methods (*i.e.*, high pressure homogenization, high shear turbulence) to form ultra-fine droplets. There is often a slight difference in size domains between the two, in that nanoemulsions may encompass a slightly larger size distribution, often 200 nm or less, but up to 500 nm have been described (McClements, 2012).

Since there is no defining surfactant concentration separating nanoemulsions from microemulsions, the characterization and differentiation between the two is often a delicate task. Employing the so-called dilution method is applicable to many systems and provides very clear differentiating behaviour that sets the two apart. Upon addition of a diluent, nanoemulsions do not typically undergo a transition to a S3 or S1/S2 microemulsion phase. Rather, they simply phase

invert from w/o to o/w or *vice versa* as the diluent concentration increases. This nanoemulsion phase inversion is normally preceded by growth in droplet diameter (McClements, 2012). Microemulsions can consist of very complex phase diagrams, including but not limited to, S1-S4 microemulsion regimes and liquid crystalline phase and transitions (Friberg, 1985; Quemada & Langevin, 1985; Winsor, 1948). This is especially true for microemulsions using monoglycerides as a primary surfactant, as these are small molecules that effectively organize into numerous forms and readily transition into others given the inherent flexibility of their packed films (Engstrom, 1990; Guillot *et al.*, 2006; Parris, Joubran, & Lu, 1994; Sagalowicz *et al.*, 2006). As well, there may be transitions from a liquid crystalline phase to a reverse micelle (L2) phase by increasing the temperature of a monoglyceride-based microemulsion (Amar-Yuli & Garti, 2005; Guillot *et al.*, 2006; Sagalowicz *et al.*, 2006).

Typically, thermodynamic stability has been considered tantamount to shelf stability. In this regard, microemulsions are often identified by their ability to remain in storage for extended periods of time without phase separation or change in droplet size, presuming no change in environmental conditions or breakdown due to external factors (light, temperature, shear, *etc.*). Nanoemulsions may phase-separate over time or exhibit droplet growth through coalescence (McClements, 2012). Although a reliable method to determine thermodynamic stability, the timeframe necessary to make such claims is quite lengthy. While this method best reflects behaviour under shelf storage conditions, more rigorous conditions such as centrifugation can be used to induce destabilization in a shorter timeframe.

1.3.4 APPLICATIONS OF MICROEMULSIONS

Numerous studies have indicated the potential for microemulsions to be effective in controlled release in nutraceuticals and pharmaceutical packaging, but as yet, few consumer products exist in microemulsion form, likely owing to the high concentration of surfactant(s) and

co-surfactant(s) in the system (Lawrence & Rees, 2000; Rozman & Gasperlin, 2007; Spornath & Aserin, 2006).

A commercially available microemulsion-based pharmaceutical is Neoral™. It consists of Cyclosporin A, an immunosuppressive agent used in post-organ transplants and is poorly water-soluble (Gao *et al.*, 1998). Decades ago, Cyclosporin A was dissolved in vegetable oil capsules and showed variable release kinetics, which rendered it less effective. Encapsulating this drug within a w/o microemulsion proved to be highly advantageous as there have been various reports showing that this formulation provides superior absorption rates and systemic availability over previous drug delivery methods (Mueller *et al.*, 1994). The mode of release is assumed to be through phase inversion from w/o to o/w upon exposure to water (Lawrence & Rees, 2000).

1.4 EMULSIFIED MICROEMULSIONS

As previously mentioned, DEs consist of an internal emulsion dispersed within a second continuous phase to form an emulsion within an emulsion. An area of growing interest is that of spontaneously-formed internal phases where the inner emulsion is generated *via* self-assembly. The vast majority of self-assembled inner phases have consisted of liquid crystalline phases (Yaghmur & Glatter, 2009). Their formation is largely dependent on composition (Kulkarni, Mezzenga, & Glatter, 2010; Larsson, 1991; Libster, Aserin, Yariv, Shoham, & Garti, 2009; Pilman, Karsson, & Tornberg, 1980; Salonen & Glatter, 2010; Yaghmur, Campo, & Glatter, 2008; Yaghmur *et al.*, 2005; Yaghmur, Campo, Sagalowicz, Leser, & Glatter, 2006; Yaghmur, Rappolt, Østergaard, Larsen, & Larsen, 2012; Yaghmur & Glatter, 2009), but may also be governed by temperature (Guillot *et al.*, 2006). The first recorded instance of a thermodynamically-stable nanostructured dispersion within an aqueous matrix was described by Pilman *et al.* (Pilman *et al.*, 1980). This system was composed of glycerol monolaurate as the emulsifier, water and either soybean or sunflower seed oil for the oil phase. The L2 phase was further dispersed within a 2.5% sodium

caseinate solution using high shear homogenization (Larsson, 1991; Pilman *et al.*, 1980) which was stable for up to 3 days. This group did not perform extensive structural studies on the so-named “w/o/w microemulsion emulsions”, but rather focused on the retention and release of the cationic dye methylene blue encapsulated within the reverse micellar compartment. The emulsified L2 phase had appreciable retention of methylene blue over a period of 24 hours at both room temperature and 80°C, with room temperature release studies showing that the L2 phase alone and after emulsification were similar in release behaviour (Pilman *et al.*, 1980). It was observed that during release studies, water was able to penetrate into the L2 phase, initiating a conversion into a liquid crystalline phase. It was postulated that water ingress into the L2 phase during emulsification with sodium caseinate could also produce such transitions, but when considering the short timescale of the emulsification process, this effect was deemed negligible. It was concluded that emulsification of the L2 phase was successful and that it maintained its structure after emulsification, though no subsequent investigation was performed to corroborate this hypothesis. A study performed in 2009 by O’Regan and Mulvihill indicated that methylene blue release from DEs has historically been variable in its recovery as the cationic dye may readily interact with proteins such as caseins (Regan & Mulvihill, 2009). Pilman *et al.* did, however, speculate on the L2 structure of the ‘microemulsion emulsion’ and inferred that the microemulsion structure consisted of flattened disk-like structures containing the monoglyceride-stabilized water phase surrounded by the oil phase (Pilman *et al.*, 1980).

As well, a patent on self-emulsifying $w_1/o/w_2$ multiple emulsions has been submitted (Goankar, 1994). The terms of the patent presented compositions inconsistent with food applications, namely the use of high alcohol-based co-surfactant concentrations (Lutz *et al.*, 2007). Nevertheless, this patent demonstrated that the use of a thermodynamically-stable microemulsion phase residing within emulsion droplets is a promising controlled release option that warrants further study.

More recently, Yaghmur *et al* formulated water-tetradecane-glycerol linoleate-based microemulsions dispersed within a triblock co-polymer (Yaghmur *et al.*, 2005). These ‘emulsified microemulsions’ were stable for up to 4 months and characterized using Cryo-TEM (transmission electron microscopy) and small angle x-ray scattering (SAXS). These studies also confirmed that there was no structure loss during storage over months. A structural depiction of this system is shown in Figure 3. This study, as well as that of the Guillot research group confirmed that the emulsified liquid crystalline phases were tunable in response to temperature, transitioning into emulsified microemulsions with an increase in temperature (Guillot *et al.*, 2006; Yaghmur *et al.*, 2005).

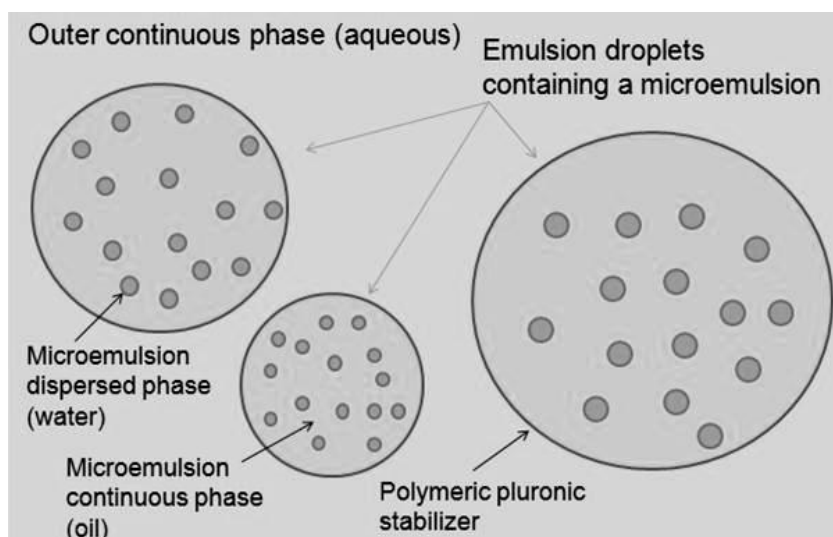


Figure 3 - Emulsified microemulsion domains as described by Yaghmur *et al.*, 2005.

Lutz *et al.* (Lutz *et al.*, 2007), conducted studies on compositionally-different microemulsions and corroborated the SAXS findings observed by the Yaghmur research group. The microemulsion was a 5-component mixture also stabilized by a tri-block copolymer. The structural information obtained from this study coincided with those reported by Yaghmur where the internal

disorder of the microemulsion system persisted after emulsification. In both studies, it was observed that the single broad peak observed through SAXS, termed the 'characteristic distance', shifted to higher d-spacings, corresponding to increased order in the system after emulsification (Yaghmur *et al.*, 2005). There was also speculation that the polymeric stabilizer increased the order of the dispersed microemulsion given the presence of localized ordering at the droplet interface between the interfacially-bound monoglyceride and polymer (Lutz *et al.*, 2007).

1.4.1 EMULSIFIED MICROEMULSION FORMULATIONS

These dispersions formally named and described in detail in 2005 (Yaghmur *et al.*, 2005) were categorized under the newly coined term, ISAsomes, standing for Internally Self-Assembled particles, or “somes”, which we now consider a synonym to emulsified microemulsions (EMEs). These consisted of glycerol monolinoleate, tetradecane and water comprising the microemulsion phase. This was then dispersed in an aqueous outer phase and its droplets stabilized by a triblock co-polymer (Yaghmur *et al.*, 2005; Yaghmur & Glatter, 2009). This composition was able to accommodate approximately 5-11% w/w water into the microemulsion inner phase. The microemulsion and EME were formed using ultrasonication in a “one-pot” approach. EMEs were stable over a period of 4 months, showing no changes to the microemulsion component or the overall emulsion. The research group also formulated food-grade EMEs (Yaghmur & Glatter, 2009), but did not expand on their applications. Other groups have reported similar results with monolinoleate-based EMEs and have shown that the inner structure is sensitive to temperature (Guillot *et al.*, 2006) and component mass ratios (Lutz *et al.*, 2007; Yaghmur *et al.*, 2005; Yaghmur & Glatter, 2009).

Applications using EMEs formed using monoglycerides are restricted by their limited water content, as they can only incorporate a maximum of ~15% w/w water within the L2 phase (Yaghmur *et al.*, 2005). This ultimately lowers the loading capacity of a desired compound within

the inner aqueous dispersed phase. However, this phase may be advantageous over 2D crystalline structures such as the reverse-hexagonal phase in terms of inner aqueous phase retention since there are no channels present in the L2 phase through which the desired compound can escape. As a result, such a limited connection with the outer aqueous phase may prove beneficial for long term shelf storage and improved control of release patterns (Sagalowicz *et al.*, 2006).

1.4.2 CHARACTERIZATION

There is no standardized technique to characterize microemulsions. Two commonly-used methods are SAXS and Cryo-TEM as they permit identification of some of their structural features at the nano-scale.

1.4.2.1 SMALL ANGLE X-RAY SCATTERING (SAXS)

Nanostructured emulsions require characterization methods that show structure at the nanometre and Ångstrom length scales. SAXS was extensively used in Yaghmur's comprehensive EME characterization study and in others concerning nanostructured dispersions (Guillot *et al.*, 2006; Lutz *et al.*, 2007; Yaghmur *et al.*, 2008, 2005; Yaghmur & Glatter, 2009).

In SAXS, the elastic scattering of X-rays ($\lambda \sim 0.1\text{-}0.2\text{ nm}$) recorded at very low angles ($< 10^\circ$) yields key information such as the size/shape of macromolecules and characteristic length scales between ~ 5 and 150 nm , depending on how (dis)ordered the system is (Feigin & Svergun, 1987; Koch, 2006; Teubner & Strey, 1987).

Concentrated systems (*i.e.* those that contain a high concentration of scattering bodies in close proximity) create great deal of multiple scattering. This is due to diffracted waves impinging on adjacent scatterers, creating secondary waves. Ideally, dispersed samples studied using SAXS should be dilute systems to prevent secondary scattering (Koch, 2006).

Winsor Type IV microemulsions are inherently disordered systems that only yield a broad scattering peak on a SAXS diffractogram (Fanun, 2009a, 2009b; Lutz *et al.*, 2007; Teubner & Strey, 1987). The scattering peak is referred to as the “characteristic distance” (Lutz *et al.*, 2007; Teubner & Strey, 1987; Yaghmur *et al.*, 2005) as the microemulsion structure lacks distinct planes and thus periodicity. Since the droplets dispersed within a microemulsion are within the size domain observable by SAXS, this information indicates little beyond the increase or decrease of order within the system, however, the characteristic peak does appear to persist after emulsification with polymeric stabilizers (Larsson, 1991; Lutz *et al.*, 2007; Yaghmur *et al.*, 2008). Since there are no distinct scattering planes, the broad peak corresponds to an average distance between scatterers, with its broadness reflecting the wide distribution of inter-particle distances.

1.4.2.2 CRYO-TEM

In transmission electron microscopy (TEM), an electron beam is focused and directed through a thin film sample by several magnetic lenses, with part of the beam adsorbed or scattered by the sample while the remaining is transmitted. The transmitted electron beam is magnified and then projected onto a screen to generate an image of the specimen. The fraction of electrons transmitted depends on sample density and film thickness. Optimal film thickness is between 10-100 nm to allow for electrons to pass through the sample with minimal back scattering interference (Ayache, Beunier, Boumendil, Ehret, & Laub, 2010).

Sample preparation techniques greatly influence the resolution of the observed images. Sample treatment by staining with contrast agents containing electron-rich heavy metal compounds such as uranyl acetate, phosphotungstic acid or osmium tetroxide (OsO_4) helps to reveal the presence of smaller particles such as microemulsion domains (Ayache *et al.*, 2010). In particular, OsO_4 is active at C=C bonds, which is particularly advantageous in imaging unsaturated

monoglyceride-based dispersions (Ayache *et al.*, 2010; Vrignaud, Anton, Gayet, Benoit, & Saulnier, 2011).

The high vacuum used in TEM as well as sample preparation techniques can lead to possible structure alteration or collapse (Ayache *et al.*, 2010). In order to overcome these problems, alternative methods such as Cryo-TEM have been employed, where samples are quench-frozen to minimize structural damage (Ayache *et al.*, 2010; Sagalowicz *et al.*, 2006; Vrignaud *et al.*, 2011). This technique was originally developed to maintain the structural integrity of complex biological samples, but can be applied to structured, non-biological specimens (Ayache *et al.*, 2010).

Imaging of individual structured emulsion droplets can give direct evidence of their internal architecture (Sgalowicz *et al.*, 2006). For example, in an emulsion droplet consisting of a liquid crystalline matrix, the internal dispersed droplets will arrange themselves in a distinct ordered arrangement. For example, in an H₂-containing droplet, the internal droplets appear in a honeycomb formation (*i.e.*, hexagonal mesophase). Cryo-TEM images of EMEs have shown no ordered arrangement within the droplet, further confirming that they exist as a disordered array of nano-scale droplets (Gustafsson, Ljusberg-Wahren, Almgren, & Larsson, 1997; Lutz *et al.*, 2007; Yaghmur *et al.*, 2005).

1.5 DOUBLE EMULSIONS IN CONTROLLED RELEASE

Considerable research has been done to exploit the encapsulation capability of DEs (Dickinson, 2010a; Ficheux *et al.*, 1998; Garti & Benichou, 2004; Higashi *et al.*, 1995; Hino, Kawashima, & Shimabayashi, 2000; Kanouni *et al.*, 2002; Lutz, Aserin, Wicker, & Garti, 2009; Matsumoto, Kita, & Yonezawa, 1976; Pays, Giermanska-Kahn, Pouligny, Bibette, & Leal-Calderon, 2002; Regan & Mulvihill, 2009). By encapsulating a compound of interest within a droplet residing within a droplet, the release of this compound may be delayed or tailored to a desired release behaviour. These systems, much like EMEs, are internally structured dispersions, the major

difference being that the inner dispersion is an inherently thermodynamically-unstable emulsion, leading to coalescence and phase separation of the internal structure over time. As well, the internal phase droplets are not necessarily below 100 nm in diameter (Garti & Yuli-Amar, 2008; McClements, 2012).

Release of encapsulated compounds within fine droplets may occur through a process known as “reverse micellar transport” where similarities in solubility between the internal dispersion and the outer continuous phase cause the fine internal droplets to diffuse to the external phase (Ficheux *et al.*, 1998; Garti & Benichou, 2004). Since the merging of small droplets with larger ones is a thermodynamically-favourable process, the small internal droplets are thermodynamically-driven to merge with the external phase, a process referred to as Ostwald Ripening (Ficheux *et al.*, 1998; Kanouni *et al.*, 2002; Pays *et al.*, 2002). Compounds encapsulated within the internal compartment are released into the continuous phase. This phenomenon may be overcome, in part, by using a low HLB value surfactant that is irreversibly adsorbed to the w_1/o interface (Kanouni *et al.*, 2002).

Ostwald Ripening of the internal droplets with the external compartment is dependent on many factors, but most significantly on the concentration of water-soluble emulsifier in the external aqueous phase. Above a certain external emulsifier threshold concentration, the fine aqueous droplets within the oil droplet overcome the activation energy required to merge with the external aqueous phase, essentially creating a void in the surfactant monolayer (Ficheux *et al.*, 1998). This threshold value denotes the transition of the external emulsifier when it no longer provides monolayer oil droplet coverage, but rather begins to display localized agglomeration about the interface (Chen & Dickinson, 1995a, 1995b; Kanouni *et al.*, 2002). It has been found that adding an electrolyte to the w_1 phase of a $w_1/o/w_2$ DE balances the Laplace pressure within the droplet by lowering interfacial tension (Rosano, Gandolfo, & Hidrot, 1998). Ostwald ripening may also be mitigated by increasing the solute concentration of the w_2 phase. This increase in osmolarity does

not affect the migration of water between aqueous compartments provided the surfactant mix allows for the lipophilic surfactant to keep the w_1 droplets sufficiently separated from the o/w_2 interface (Wen & Papadopoulos, 2001).

Internal droplets may also coalesce with each other to form larger internal droplets over time. This form of destabilization may not necessarily result in release of the encapsulated compound which remains internalized (Dickinson, 2010a; Garti & Benichou, 2004). Internal droplet coalescence occurs if a hydrophilic emulsifier is present at concentrations within the oil droplet above a threshold value in a $w_1/o/w_2$ DE (Ficheux *et al.*, 1998; Villa, Lawson, Li, & Papadopoulos, 2003). This causes the w_1 droplets to merge into a larger droplet which is more thermodynamically-favourable.

Typically, DEs require multiple emulsifiers of differing HLB values to be formed and stabilized. This limits or prevents the migration of the surfactant stabilizing the internal droplets to the exterior phase (Ficheux *et al.*, 1998; Kanouni *et al.*, 2002). It is vital to select surfactants that not only have disparate HLB values, but also do not interact with each other (*e.g.*, through electrostatic interactions). This prevents compromising the surfactant monolayer at either the internal or external interface (Ficheux *et al.*, 1998; Garti & Benichou, 2004).

The structural properties of DEs are particularly suited for pharmaceutical purposes. In one study, the encapsulation of water-soluble Epirubicin, an anti-cancer agent, within a $w_1/o/w_2$ DE showed promise for arterial delivery in the treatment of hepatocellular carcinoma. This DE consisted of aqueous Epirubicin dispersed within iodized poppy seed oil (IPSO) and tetra-glycerine condensated ricinoleate as a surfactant (Higashi *et al.*, 1995). IPSO is a highly beneficial excipient additive for delivery directly into diseased tissue because it appears to promote tumor necrosis when used in direct arterial injection of diseased tissue (chemoembolization), although the mode of action is not well understood (Higashi *et al.*, 1995; Hino *et al.*, 2000). When combined with a chemotherapeutic agent, tumor necrosis may be enhanced, provided that the drug is successfully

deposited within the cancerous tissue. This system was capable of high drug loading and showed a prolonged residence time within the liver in rat models *in vivo* over conventional delivery methods for arterial delivery. As well, a similar IPSO-based system reported reduced toxicity on healthy liver tissue with the administration of Epirubicin in a $w_1/o/w_2$ DE, thus displaying a higher specificity for diseased tissue over non-DE formulations (Hino *et al.*, 2000).

In comparison to EMEs, DEs are prone to various destabilization phenomena that may impede the desired release or encapsulation of compounds due to the unstable nature of the internal phase. By contrast, EMEs may provide improved stability for encapsulated compounds as the internal droplets are not subject to coalescence and are less likely to merge with the external aqueous phase.

1.6 PROTEIN-POLYSACCHARIDE EMULSION STABILIZATION

Proteins are amphiphilic biopolymers that may act as stabilizers for food-grade emulsions (Dickinson, Evison, Gramshaw, & Schwoppe, 1994; Dickinson, 2010a; Jourdain, Leser, Schmitt, Michel, & Dickinson, 2008; Regan & Mulvihill, 2009). Caseins are milk proteins that stabilize micelles containing CaPO_4 nanoparticles *in vivo*. Sodium caseinate is formed by exposing purified casein to saturated NaCl, effectively displacing the calcium and forming a hydrocolloid in solution (Dickinson, 2010a). When used as an o/w emulsion stabilizer, the caseinate provides steric and electro-repulsive stabilization (Dickinson, 2001; Dickinson, 2010a,b).

Polysaccharides are normally used as thickening agents to assist in emulsion stabilization by increasing the viscosity of the continuous phase. A number of food-related polysaccharides are also known to be surface-active, namely pectin, which contains acetyl groups that enhance its hydrophobic character, rendering it somewhat surface-active (Considine *et al.*, 2011; Dickinson, Semenova, Antipova, & Pelan, 1998). Pectin is an anionic structural polysaccharide found in many kinds of fruit. It is typically used as a thickening agent and electro-repulsive stabilizer in liquid

foods (Lopes da Silva & Rao, 2006). When pectin is used in conjunction with casein, the protein and polysaccharide will form a physical complex with excess pectin forming layers surrounding this complex at the interface (Bonnet, Corredig, & Alexander, 2005; Lopes da Silva & Rao, 2006). This not only prevents coalescence of the oil droplet through steric stabilization, but also prevents bridging flocculation, an association between the proteins stabilizing adjacent oil droplets (Bonnet *et al.*, 2005; Dickinson *et al.*, 1998).

Compared to proteins or polysaccharides alone, protein-polysaccharide complexes can provide superior resistance against environmental stresses such as large changes in pH or ionic strength and typical processing operations such as thermal treatment or freezing (Considine *et al.*, 2011; Lopes da Silva & Rao, 2006). The isoelectric point (pI) of casein is 4.6 and that of pectin is ~3. As such, there is the possibility of favourable electrostatic interactions between the two at intermediate pH values. However, the casein-pectin system has been shown to be particularly suited for stabilization of continuous phases at pH 5-6 and is often used to emulsify acidified milk and yoghurt-based beverages (Dickinson *et al.*, 1998; Lopes da Silva & Rao, 2006). At such pH values, pectin, with its greater overall negative charge, is considered the anion in this complex and the interaction is electrostatically-attractive (Tuinier, Rolin, & de Kruif, 2002).

1.7 RESEARCH OBJECTIVES

Previous studies on EMEs have either focused on their encapsulating ability or structure (Lutz *et al.*, 2007; Pilman *et al.*, 1980; Yaghmur *et al.*, 2008, 2006; Yaghmur & Glatter, 2009). An extensive study of their structure-function relationship has not been performed. As well, the system described by Pilman *et al.* was the only one comprised of food-grade components. Stability of the systems described by the Lutz and Yaghmur groups exhibited superior stability, but these authors did not perform an assessment of their functionality and capacity to encapsulate compounds for controlled release applications.

This thesis explored the encapsulation potential of a food-grade EME for possible use in food or pharmaceutical products and determined whether these structured emulsions were capable of acting as controlled release vehicles. The chosen system consisted of a w/o microemulsion with a monoglyceride and medium-chain triglyceride as the oily phase. The nanostructured dispersion was stabilized with a caseinate-pectin complex.

1.8 HYPOTHESES

The research hypotheses explored within this thesis were that:

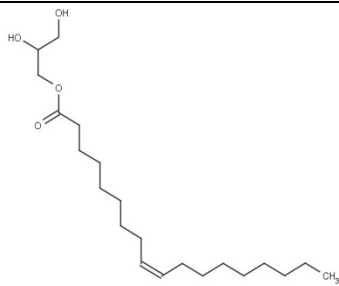
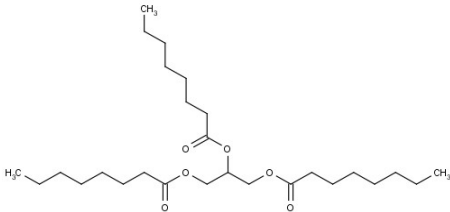
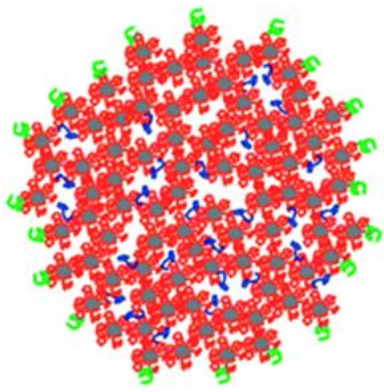
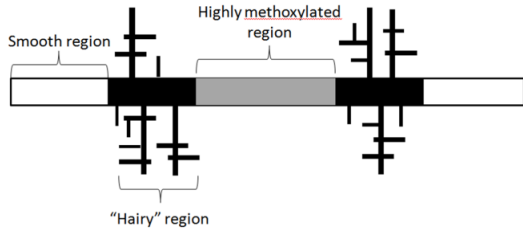
- I. A w/o microemulsion could be effectively incorporated within a continuous aqueous phase thereby resulting in an emulsified microemulsion (EME);
- II. The resulting EME could serve as a controlled release vehicle, and;
- III. The EME would be stable for an extended period of time (*i.e.*, months).

2 MATERIALS AND METHODS

2.1 MATERIALS

Monomuls 90-O18 (GMO) was donated from BASF consisting of >90% distilled monoglycerides (>80% glycerol monooleate). Pectin (Genu® Pectin) was a gift received from CP Kelco, Denmark. Tricaprylin (TC, ≥99% purity) and bovine casein sodium salt (NaCas) was purchased from Sigma-Aldrich. All water was nanopore-filtered reverse osmosis water. The materials used and their respective structures are depicted in Table 1.

Table 1: Constituent reagents and chemical structures used in this study to form food-grade EME.

Component	Structure	Function
Glycerol Monooleate		Lipid-tending surfactant, stabilizes water droplets within microemulsion compartment of EME (Yaghmur <i>et al.</i> , 2005)
Tricaprylin		Neutral, medium-chain triglyceride, part of oil phase in microemulsion compartment of EME (Pilman <i>et al.</i> , 1980)
Sodium Caseinate		24 kDa glycosylated peptide. Complexes with polysaccharide to stabilize oil droplets (Dickinson, 2001), Mixture of the α_s1 , α_s2 , β and κ casein forms. Representation from (Dalglish, 2011).
Pectin		Branched, anionic polysaccharide, complexes with casein. Increases viscosity of EME aqueous continuous phase. Adapted from (Lopes da Silva & Rao, 2006)

2.2 MICROEMULSION FORMULATION

GMO and TC were heated together in a 1:1 mass ratio to 60°C and mixed at constant temperature by magnetic stir bar for 10 minutes at 500 RPM. A 9.5 g sample of the 1:1 GMO:TC mixture was transferred to a rinsed and dried glass test tube. A small amount (0.5 g) of 60°C water was added to the test tube, capped and immediately mixed by vortex mixer at 3000 RPM for 30 seconds. The mixture was then permitted to equilibrate at room temperature for 24 hours. The resulting homogeneous solution was a 5% w/o microemulsion by mass and constituted the oil component of the EME. The microemulsion used in the methylene blue release tests was prepared in the same manner, but contained 0.1950 g methylene blue/100 g water within the aqueous phase.

2.3 EMULSIFIED MICROEMULSION FORMULATION

Stock solutions of 2% w/w sodium caseinate (NaCas) and 6% w/w pectin were prepared by mixing each of the dry biopolymers separately with the appropriate amount of water in stoppered glass flasks to prevent evaporation following by mixing with a magnetic stir bar at 500 RPM overnight. An aqueous continuous phase was prepared by mixing equal mass quantities of the NaCas and pectin stock solutions, giving final continuous phase concentrations of NaCas and pectin of 1% w/w and 3% w/w, respectively.

The 5% w/o microemulsion was emulsified to form an EME using a membrane emulsification unit (MicroPore Technologies, Derbyshire, UK). A schematic of this membrane emulsification system used is shown in Figure 4.

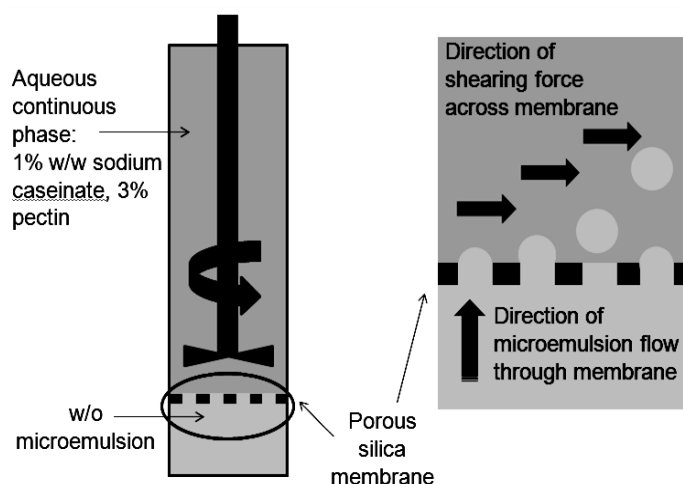


Figure 4 - Schematic of membrane emulsification unit and mode of action. Left, lateral view of membrane emulsification unit. Right, oil droplets exiting pore outlets.

This emulsification system provides ‘gentle’ dispersion of an oil phase into an aqueous continuous phase. By emulsifying with minimal energy, there is a greater probability of maintaining emulsion droplet nanostructure. By passing the dispersed phase through the porous membrane, the surfactant stabilizer wets the oil-interface, allowing for slow and even coverage of the oil droplets by the lipophilic stabilizer. As the nascent droplets exit the membrane surface, shear forces dislodge the droplet from the pore outlet which is then dispersed into solution. High energy input is not required for this method as the droplet formation is dependent on dispersed phase flow rate, membrane pore size and continuous phase viscosity, but not turbulent flow, to cause dispersed phase deformation and fragmentation (Joscelyne & Trägårdh, 2000). The microemulsion droplets remain suspended within the oil phase. This method has been previously employed for DE formation (Hino *et al.*, 2000; Joscelyne & Trägårdh, 2000; Nakashima, Shimizu, & Kukizaki, 2000).

A 10 μm pore diameter silica-coated membrane was cleaned and prepared according to manufacturer instructions (Ultrasonication for 30 seconds in each of the indicated media in the

following sequence: 4M NaOH (aq), water, 2% w/w citric acid, water, 1:5 continuous phase diluted with water). The membrane remained submerged in the diluted continuous phase for 30 minutes to ensure complete wetting of the membrane with the aqueous phase.

The microemulsion was added to the NaCas-pectin continuous phase at a rate of 1 mL/min, passing through the wetted membrane. The required shear force was provided by motorized propeller corresponding to approximately 1250 RPM. The resultant white emulsion was subjected to characterization by droplet size distribution, zeta potential, SAXS, Cryo-TEM and DSC. This procedure was repeated on an oil phase consisting of 1:1GMO:TC free of solubilized water to act as a blank emulsion standard.

EMEs loaded with methylene blue-containing microemulsions (MBEMEs) were prepared as described above for the determination of encapsulation efficiency. A blank emulsion standard was prepared with an equivalent amount of methylene blue on a w/w basis in the external aqueous phase to simulate complete release of methylene blue from the internal aqueous compartment. These are henceforth referred to as MBEs.

2.4 CHARACTERIZATION

2.4.1 DROPLET SIZE DISTRIBUTION

The droplet size distributions of the outer emulsions used to form the EMEs were determined using a Mastersizer 2000S particle size analyser (Malvern Instruments, Worcestershire, UK) at a stir rate of 1000 RPM and exposure time of 20 seconds/measurement. The average of 10 measurements was taken per sample on 3 separate samples.

2.4.2 ZETA POTENTIAL

EME zeta potential was performed on a 90Plus particle size analyzer with a Zeta PALS zeta potential module (Brookhaven Instruments Corporation, New York, USA). Emulsified

microemulsion and emulsion samples were diluted with nanopore filtered water and subjected to 5 cycles at 25 °C.

2.4.3. INVERTED LIGHT MICROSCOPY

Emulsion droplets were observed for particle size and shape using an inverted light microscope. Images of emulsion samples were observed at a magnification of 1008 X using a Zeiss Axiovert 200M inverted light microscope (Zeiss Canada, Toronto, ON, Canada). Images captured on CCD camera were analyzed with Northern Eclipse software, Version 7.0. (Empix Imaging, Inc., Mississauga, ON, Canada).

2.4.4. SMALL ANGLE X-RAY SCATTERING

SAXS of the EMEs, blank emulsion and dispersed phases was investigated using a Hecus S3-MicroCalix® SWAXS-DSC high flux system (Hecus, Graz, Austria). The unit uses a 50 W, high brilliance GeniX microfocus source and customized FOX-3D multi-layer point focusing optics (Xenocs SA, Grenoble, France) with a 100 x 250 μm^2 FWHM (vertical x horizontal) at focus. The x-ray beam was generated by a 50 kV, 1 mA Cu K α anode ($\lambda = 1.546 \text{ \AA}$). The sample-detector distance was ~280 mm (SAXD) and ~300 mm (WAXD). Scattering data were captured with dedicated Hecus 1-D position-sensitive detectors (model PSD-50M). The SAXS X-ray range was $2000 \text{ \AA} > d > 11 \text{ \AA}$. For sample preparation, ~20 μL of sample were placed in 1.5 mm O.D. quartz capillaries (Charles Supper Company, Inc., Natick, MA, USA) using a long needle and syringe. The sample was then transferred to the unit's sample port and analyzed at 25°C for 16 hrs. Calibration was performed using silver behenate for the SAXD region with bromobenzoic acid. Data was analyzed using EasySWAXS and 3Dview software to determine d spacing/characteristic distances.

2.4.5. DIFFERENTIAL SCANNING CALORIMETRY

A Pyris Diamond differential scanning calorimeter (DSC) (Perkin Elmer, Massachusetts, USA) was used to measure enthalpic changes and transition temperatures of EMEs, emulsions, dispersed phases and single components. Each sample (3-6 mg) was placed in an aluminum pan (20 μ L capacity) and hermetically sealed with a sample press. All measurements were conducted between 40°C to -70 °C at a constant rate of 5°C/min with a holding time at each boundary temperature for 5 minutes.

2.4.6. CRYO-TRANSMISSION ELECTRON MICROSCOPY

Cryo-TEM of the 5% w/o microemulsion was performed at McMaster Children's Hospital (Hamilton, ON, Canada) using the following procedure: A 3.4 μ L droplet of sample was placed on a Formvar-coated grid for 2 minutes and the excess sample wicked away with filter paper. The grid was placed in a covered Petri dish with \sim 1ml of 2% aqueous OsO₄. Vapours from the OsO₄ stained the hydrophobic phase of the microemulsion. The treated sample was then observed under low dose conditions using a JEOL 1200 EX TEM equipped with a Cryo-holder and images taken with a 4 megapixel CCD camera.

Imaging of the EME was performed at the University of Guelph (Guelph, ON, Canada) using the following procedure: EME samples were diluted 1/100 in filtered double distilled H₂O to a final concentration of 0.2% (w/v). Diluted samples (\sim 7 μ L) were loaded onto plasma cleaned copper QUANTIFOIL® Multi A grids (Electron Microscopy Sciences, USA) and plunge-frozen in liquid ethane using a manual plunge freezing device. Frozen samples were maintained at liquid nitrogen temperatures prior to loading in Gatan 914 High Tilt Liquid Nitrogen Cryo Transfer Tomography Holder (Gatan Inc., USA). Samples were imaged the same day using the Technai G2 F20 microscope (FEI Co., Netherlands) equipped with a field emission gun operating at 200kV and a 4kx4k charge-

coupled device camera. High magnification images were taken at 92,000X magnification at spot size of 6.

2.4.7. RELEASE BEHAVIOUR

Release studies of MBMEs and MBEMEs were performed by loading samples into rinsed dialysis tubing (7Spectra/Por®, Spectrum Laboratories, Inc., 10000 Da size cut-off, 24 mm diameter cellulose membrane) and sealed. These samples were then placed into a release medium consisting of distilled water containing 0.01% sodium azide (>99.5%, reagent grade, Sigma-Aldrich) to prevent microbial contamination and stirred at 50 RPM continuously. Three (3) mL samples of the release medium were taken and replaced to maintain volume continuity every 1 hr for 4 hrs, then at 20, 24, 44 and 48 hours. Methylene blue concentration was determined using a UV/Vis spectrophotometer (Lambda 40, Perkin-Elmer, Massachusetts, USA). Sample absorbance was measured at 665 nm. All samples were performed in triplicate.

2.4.8. STATISTICAL ANALYSIS

All experiments were performed in triplicate and the results were analyzed by Analysis of Variance with Least Significant Difference at a 95% confidence interval. Results shown are average \pm standard deviation and are considered significant at $p < 0.05$.

RESULTS AND DISCUSSION

2.5. MICROEMULSION FORMULATION

A time/temperature-equilibrated ternary phase diagram of water, tricaprylin and GMO at different weight ratios was used to delineate the composition of these three constituents leading to the formation of w/o microemulsions (Fig. 5). The region nestled along the tricaprylin/GMO axis at low water content resulted in an optically clear, isotropic, homogeneous regions considered to be the desired microemulsions. Confirmation of the Winsor IV region was performed by diluting the microemulsion with extra volumes of water phase until two or more phases were visible. Beyond the microemulsion region, samples examined through polarizing filters showed birefringence, indicating either liquid crystalline or bicontinuous structures within.

As per previous studies, such complex phase behaviour was expected for GMO-based microemulsions. As well, a small L2 region is typical for ternary systems that do not contain co-surfactants such as small-chain alcohols. Microemulsions falling within the single phase region of the ternary phase diagram were stable for at least 1 year at room temperature without phase separation.

Microemulsions formed along dilution line 5:5 exhibited the highest water holding capacity, ~5% w/w. Microemulsions formed at higher GMO:TC ratios, up to 8:2 GMO:TC, but could only accommodate up to 3% water content and formed a Winsor III microemulsion upon further addition of water. Phase separation of the oil and water phases formed at GMO:TC ratios of 4:6, forming crystalline sediments upon addition of ~5% w/w water content. This low water capacity was consistent with monoglyceride-based microemulsions (Guillot et al., 2006; Larsson, 1991; Pilman et al., 1980; Pilman, Tornberg, & Larsson, 1982; Sagalowicz et al., 2006; Yaghmur et al., 2008, 2005, 2006, 2012; Yaghmur & Glatter, 2009). Microemulsions containing 5% w/w water

formed at room temperature along dilution 5:5 were used in constructing EMEs as the surfactant was in excess at this dilution.

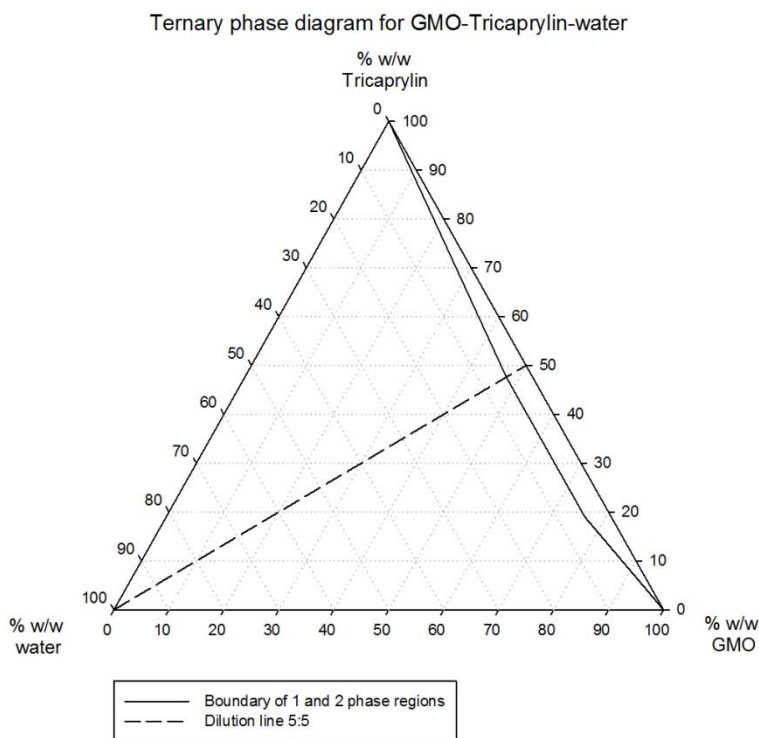


Figure 5 - Ternary phase diagram for the glycerol monooleate (GMO)-tricaprylin-water system at room temperature. The microemulsion region is shown along the GMO-tricaprylin axis. The dotted line corresponds to the 5:5 dilution line used for formulating the microemulsions and EMEs used in this study.

Cryo-TEM of a 5% w/o microemulsion showed clustered spherical water droplets residing in an oil phase (Fig. 6). Cryo-TEM of the oil phase as a control showed no droplets (not shown). It is clear that water was successfully dispersed within the oil phase at dilution line 5:5 and yielded a Winsor IV structure. No ordered crystalline structure was observed.

Image analysis was carried out using ImageJ software (National Institutes of Health Research Services Branch, Version 1.48a Released July 2013). The image was treated with

background subtraction and watershed to separate poorly resolved droplets after transforming to a binary image. Diffuse, dark regions corresponding to remaining background were cleared and not considered in particle size calculations. Particle analysis yielded a droplet diameter of 15 ± 9 nm which is consistent with microemulsion droplet size domains.

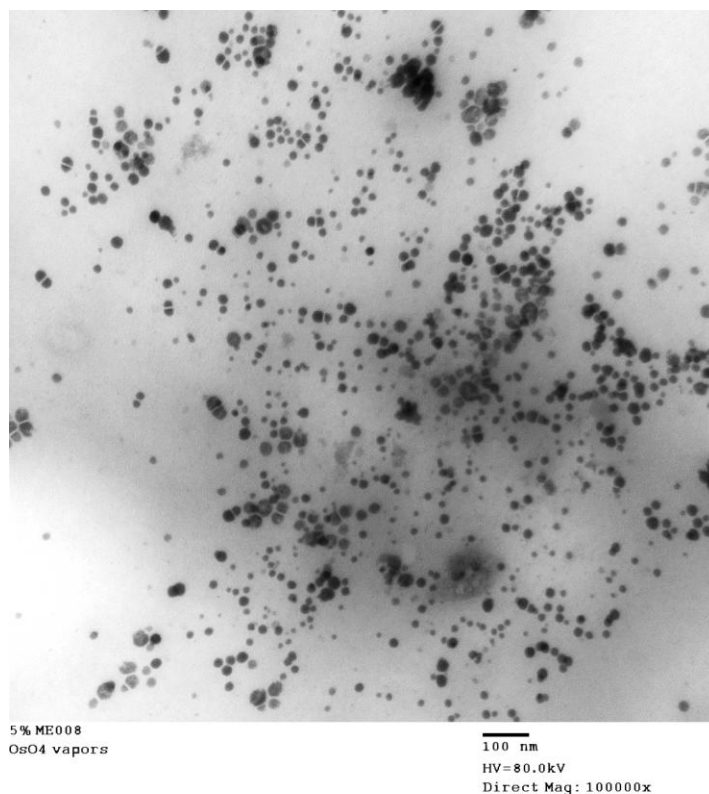


Figure 6 - Cryo-TEM image of OsO_4 -stained w/o microemulsion droplets.

2.6. EME STABILITY, DROPLET SIZE DISTRIBUTION AND ZETA POTENTIAL

When using membrane emulsification, parameters such as rotational speed (RPM) can be used to control the size of the resulting emulsion droplets (Joscellyne & Trägårdh, 2000). A rotational speed of ~ 1200 RPM yielded consistent droplet sizes, as discussed in the following section. A pectin:NaCas ratio of 3:1 w/w provided the highest dispersion capacity. EME and

corresponding control emulsions (i.e., no internal microemulsion, only dispersed water) could not contain more than 25% dispersed phase as the membrane emulsification unit was unable to overcome the increasing viscosity with an increase in the concentration of the dispersed phase. Concentrations higher than 25% oil phase content separated immediately after emulsification. This was likely due to incomplete wetting of the oil droplets with the protein-polysaccharide complex. Incompletely-covered droplets are more likely to undergo coalescence which leads to creaming and phase separation (Dickinson, 2001; Dickinson, 2010a).

Light microscopy was used after emulsifying (day 0) to verify that the membrane emulsification system yielded o/w dispersions (Figure 7). It is clear that the oil phase in both the EME and emulsion was successfully emulsified using this system.

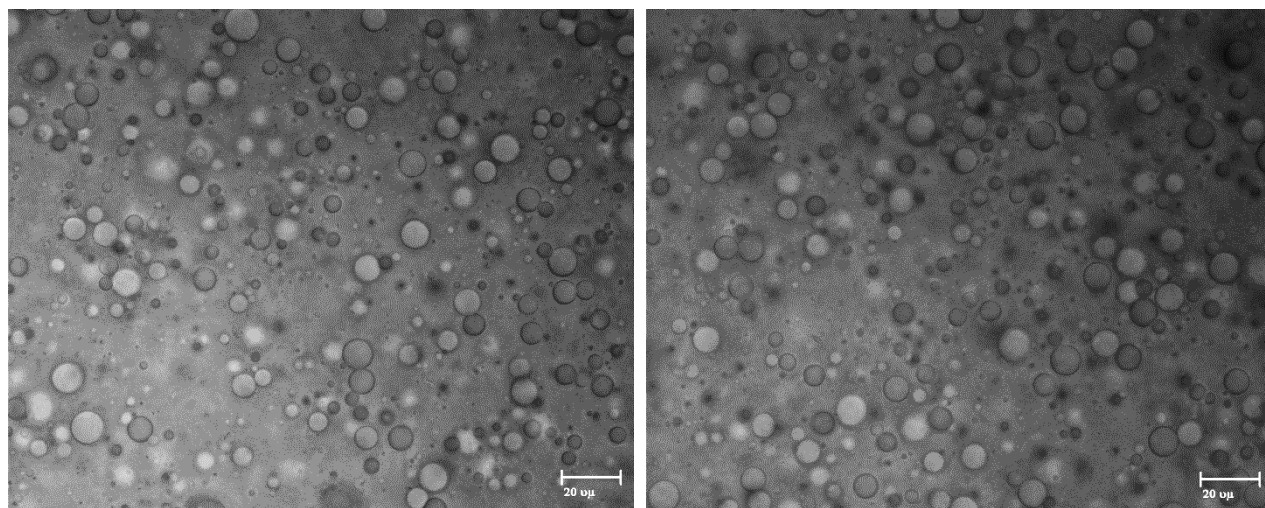


Figure 7 - Light microscopy images of 1:3 casein-pectin stabilized dispersions on Day 0 at 630 X under oil immersion. Left: 15% $w_1/o/w_2$ EME, Right: 15% o/w emulsions. Bar = 20 μ m.

Droplet size determination and zeta potential were performed on emulsions and EMEs aged up to 14 days to monitor stability during room temperature storage. After day 14, all samples

exhibited visual phase separation by creaming and were no longer characterized for their droplet size. Droplet size distributions are shown in Figure 8.

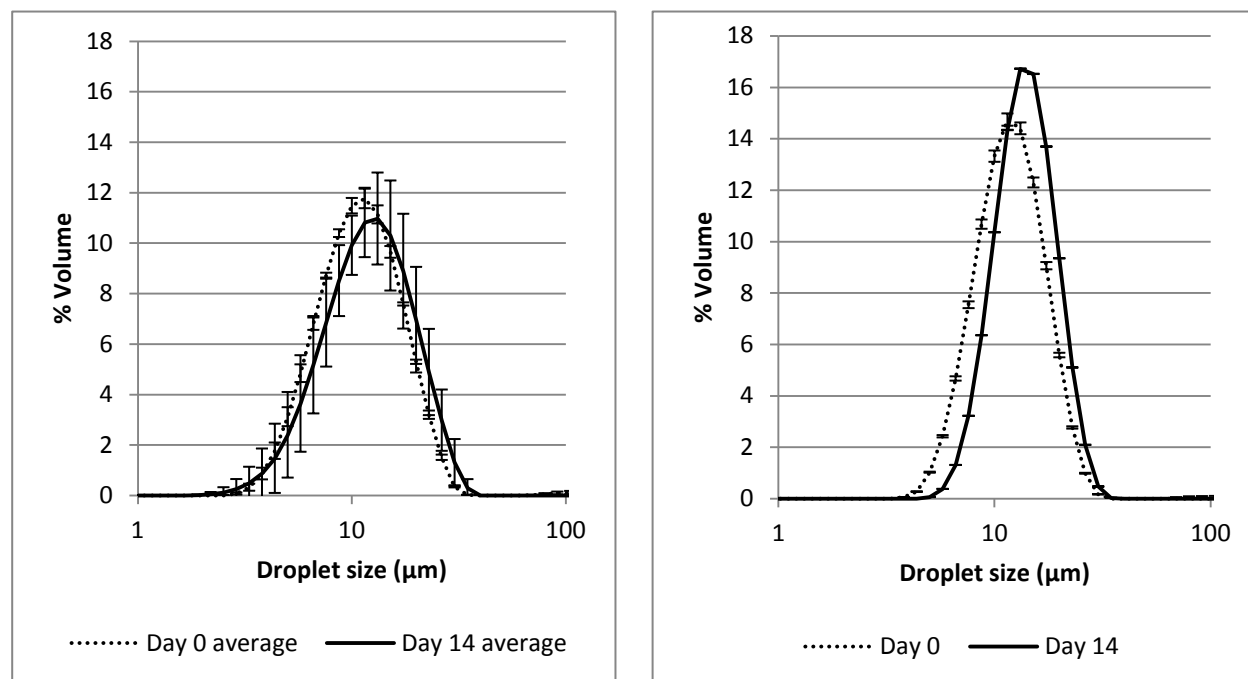


Figure 8 - Droplet size distribution of 18% w/o/w EME and 20% o/w emulsion after 14 days of ageing at room temperature.

The volume-weighted mean diameter ($d_{4,3}$) of the EME immediately following preparation (day 0) was $13.0 \pm 1.5 \mu\text{m}$ and on day 14, it was $15.8 \pm 3.6 \mu\text{m}$ ($p > 0.05$) (Figure 8). The average $d_{4,3}$ of the emulsion was $11.6 \pm 0.1 \mu\text{m}$ on day 0 and increased significantly to $13.5 \pm 0.0 \mu\text{m}$ after 14 days ($p < 0.001$), indicative of coalescence.

The zeta potential, which is the electric potential across an interface, was measured for the blank emulsions and EMEs. A high absolute value indicates a charged surface, causing electrostatic repulsion between adjacent droplets (Hanaor, Michelazzi, Leonelli, & Sorrell, 2012). A zeta potential value close to zero indicates a global surface charge of zero and as a result, stabilization of

droplets in an emulsion is not caused by electrostatic repulsion. The EME zeta potential measured immediately after membrane emulsification yielded an average value of -38.2 ± 3.3 mV and of -35.2 ± 4.4 mV after 14 days of storage at room temperature ($p > 0.05$). The zeta potential of the emulsions had an average value of -40.1 ± 0.0 mV and remained effectively the same on day 14, measuring -38.2 ± 13.2 mV ($p > 0.05$). The highly negative zeta potential values indicated that there was electrostatic stabilization of the EME and emulsion droplets (Dickinson *et al.*, 1998; Lopes da Silva & Rao, 2006; Tuinier *et al.*, 2002).

Negative zeta potentials as seen here are consistent with an emulsion stabilized by a casein-pectin complex. In this scenario, stabilization was provided through steric and electrostatic repulsion, thereby keeping the oil droplets separated, thus preventing coalescence. The large negative zeta potential values were likely due to the pectin shell surrounding the casein-stabilized droplets as pectin carries a negative charge at pH ~ 5.5 (Tuinier *et al.*, 2002). Overall, there was no significant difference in zeta potential between the EME and emulsion ($p > 0.05$), which indicated that the encapsulated dispersion within the EME had no effect on overall stabilization processes. The increase in zeta potential deviation for both the EME and emulsion, however showed that at day 14, the electrostatic stabilization between emulsion droplets began to diminish, allowing for destabilization through coalescence. Such destabilization was also evident from the increase in droplet size from day 0 to day 14. Clearly, electrostatic stabilization provided by the pectin was a vital component in maintaining emulsion stability.

2.7. DIFFERENTIAL SCANNING CALORIMETRY

Constituents within a dispersion may influence enthalpic changes on various components of the system which are observable by DSC. This method monitors a change in the energy required to elicit a phase change upon heating or cooling. This is especially useful for the study of

microemulsions because free water content and interfacial water can be identified using this technique, as earlier described.

Major endotherms and exotherms are shown in Figure 9 for each of the bulk phase constituents as well as the 5% w/o microemulsion. The peaks and corresponding enthalpies for the heating and cooling cycles are summarized in Tables 2 and 3. The tables shown below summarize the enthalpic peaks of the microemulsions only and were used to calculate the free water content of the system. The 1:1 GMO:TC enthalpies were not tabulated, but are indicated in the text as there was no free water in this mixture. Individual thermograms for the microemulsion and the bulk phases are available in the appendices.

Table 2 – Summary of the heating cycle endothermic peaks for a 5% w/o microemulsion and bulk constituents. ND: Non-detectable,(n=3).

Heating regime Microemulsion			Heating regime Pure bulk phases		
	Temperature (°C)	Enthalpy (ΔH , J/g)		Temperature (°C)	Enthalpy (ΔH , J/g)
Tricaprylin	9.7 ± 0.2	102.5 ± 0.1	Tricaprylin	10.5 ± 0.1	139.7 ± 0.1
GMO	ND	ND	GMO	27.7 ± 0.0	89.8 ± 0.4
Free water	-3.6 ± 0.1	5.5 ± 0.1	Free water	3.8 ± 0.04	330.8 ± 0.3

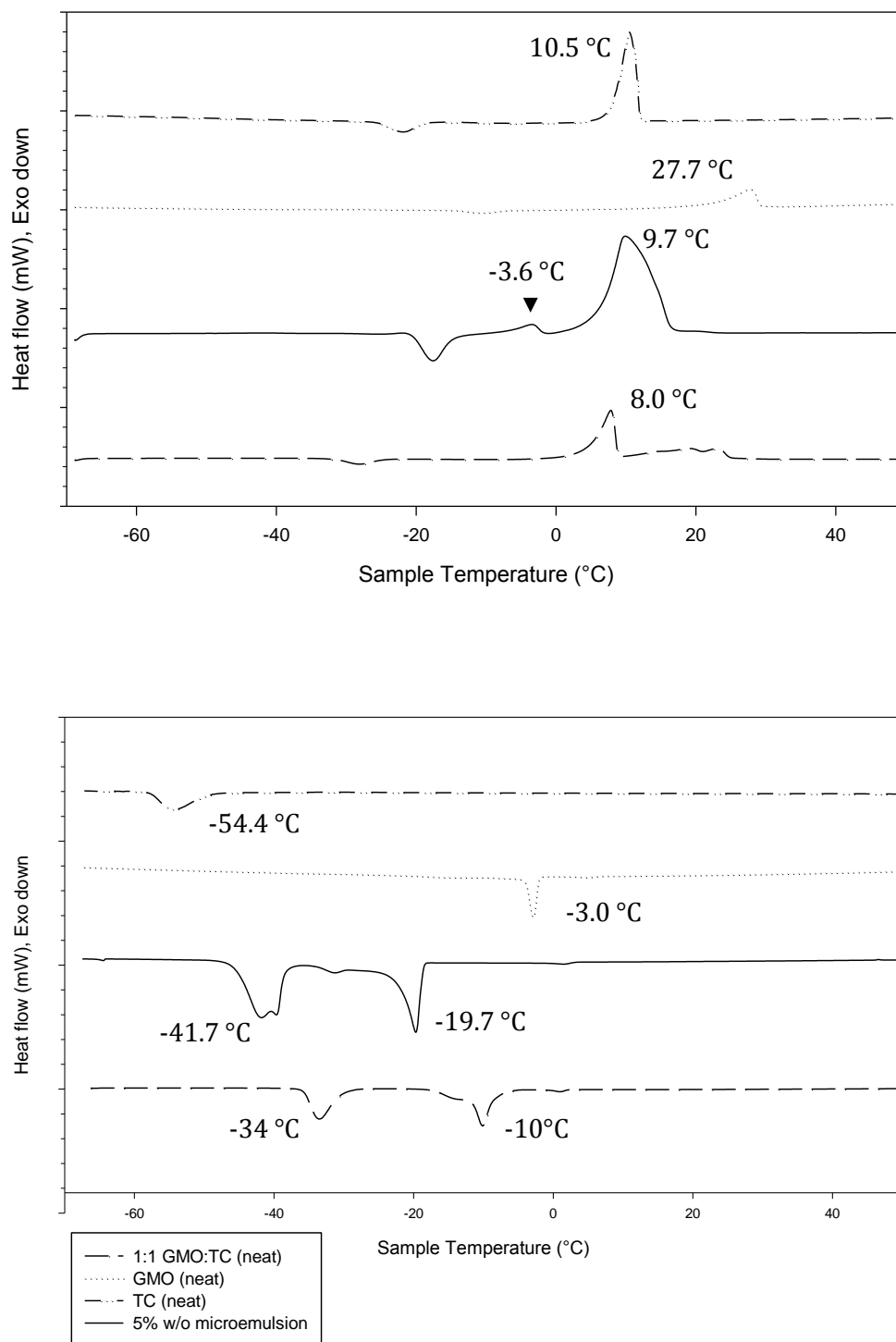


Figure 9 - Thermograms of a 5% w/o microemulsion and bulk constituents. Top: Heating, Bottom: Cooling.

Melting point depression is a colligative property that can show the effect a solute has on a solvent. This can be adapted to w/o microemulsions where the oil phase solvent is influenced by the fine water droplets which behave as a solute. By identifying the enthalpic peaks, the free water and interactions between components can be determined (Narang *et al.*, 2007; Schulz, 1998). From Figure 9, the tricaprylin melting peak shifted from 10.5 to 9.7 °C when present within a microemulsion. This behaviour was consistent with the oil phase containing solutes, in this case GMO and fine water droplets. The GMO endothermic peak was detectable in the microemulsion heating thermogram (Figure 9, Table 2), but was not reliably clear as it was small in comparison to the pure bulk phase and appeared merged with the upper temperature region of the tricaprylin peak. The GMO melting peak in the 1:1 GMO:TC mixture was quite clear (~20 °C) and did not appear to be superimposed with the TC peak at 8 °C, indicating that the two components did not complex or co-crystallize. The free water peak was quite small, but identifiable in the microemulsion thermogram at -3.6 °C.

The water core at the centre of the microemulsion water droplet will have freezing and melting points comparable to that of pure water. Using the method developed by Senatra (Senatra, 2000) for calculating the free water fraction in microemulsion samples, the fraction of free water upon heating was calculated from the peak at -4 °C. This value was at $33 \pm 1\%$ of the total water present in the system. The remainder (~67%) was considered interfacial water associated with the hydrophilic moiety of GMO, suggesting that 2/3 of the water content was 'involved' with the hydration shell around the glycerol component of surfactant at the interface. Molecular modelling studies have shown that water at least partially solvates the glycerol moiety of the surfactant and the water density within the hydration shell is slightly greater than that of water-vapour interface for lamellar GMO-based structures (Wilson & Pohorille, 1994). The interfacial thickness according to this study was calculated to be $\sim 5 \text{ \AA}$, far smaller than the interfacial water content calculated for

this system, which suggested that either the method of Senatra (Senatra, 2000) was inadequate for our purposes or perhaps that the enthalpies were not properly measured.

Table 3 – Summary of the cooling cycle exothermic peak for a 5% w/o microemulsion and bulk constituents. ND: Non-detectable (n=3)

Cooling regime Microemulsion			Cooling regime Pure bulk phases		
	Temperature (°C)	Enthalpy (ΔH , J/g)		Temperature (°C)	Enthalpy (ΔH , J/g)
Tricaprylin	-41.7 ± 0.02	-36.8 ± 0.1	Tricaprylin	-54.4 ± 0.1	-45.0 ± 0.1
GMO	-19.7 ± 0.04	-32.0 ± 0.03	GMO	-3.0 ± 0.01	-54.1 ± 0.1
Free water	ND	ND	Free water	-18.5 ± 0.4	-264.1 ± 0.8

The cooling portion of the microemulsion DSC (Figure 9, right) showed interfacial water at approximately -40°C . This temperature was consistent with the temperature corresponding to bound water (Garti *et al.*, 2000; Schulz, 1998). It was superimposed with the exothermic peak corresponding to the liquid-solid phase transition of TC. Following microemulsification, TC freezing occurred at a higher temperature ($\sim -42^{\circ}\text{C}$) than in the bulk state (-54.4°C). The microemulsified GMO and free water exothermic peaks both occurred at -18°C . As such, free water could not be identified in the cooling thermogram (ND).

The increase in the liquid-solid transition temperature of TC upon cooling was depressed for the microemulsion (-42°C) compared to neat GMO:TC, which occurred at -34°C . This was consistent with TC interacting with GMO when in a neat mixture. Though unlikely, it is possible that the GMO formed crystal aggregates throughout the system in the neat mixture but interacted with the w_1/o interface in the microemulsions, thereby preventing GMO crystallization (Frasch-Melnik, Norton, & Spyropoulos, 2010).

Figure 10 shows that the emulsion and EME melting thermograms (top) were dominated by the water peak at occurring at $\sim 2^{\circ}\text{C}$. The solid-to-liquid TC transition occurred at 8.2°C for the EME and at 8.0°C for the blank emulsion. The GMO melting peak merged with that of TC and was poorly resolved. Although there was a definite difference in the endothermic peaks of GMO upon heating in neat 1:1 GMO:TC and the 5% w/o microemulsion, this was not conserved after emulsification into either an emulsion or EME.

These cooling thermograms consisted of many narrow superimposed exothermic peaks in the range of -16 to -11°C . The peaks were not separated well enough to discern between GMO and the aqueous continuous phase. As well, the water freezing peak was too large to determine the peak locations of TC and GMO compared to the bulk, non-dispersed peaks.

Although DSC appears to be a powerful tool in characterizing microemulsions, this method was not ideal once the microemulsion or oil phase was dispersed in a secondary continuous phase given that the monoglyceride peaks provided too weak a signal at 20% w/w dispersed phase. At higher dispersed phase concentrations, the enthalpic peaks may have been better resolved, but this would have required a different emulsification method capable of producing emulsions and EMEs with higher dispersed phase contents.

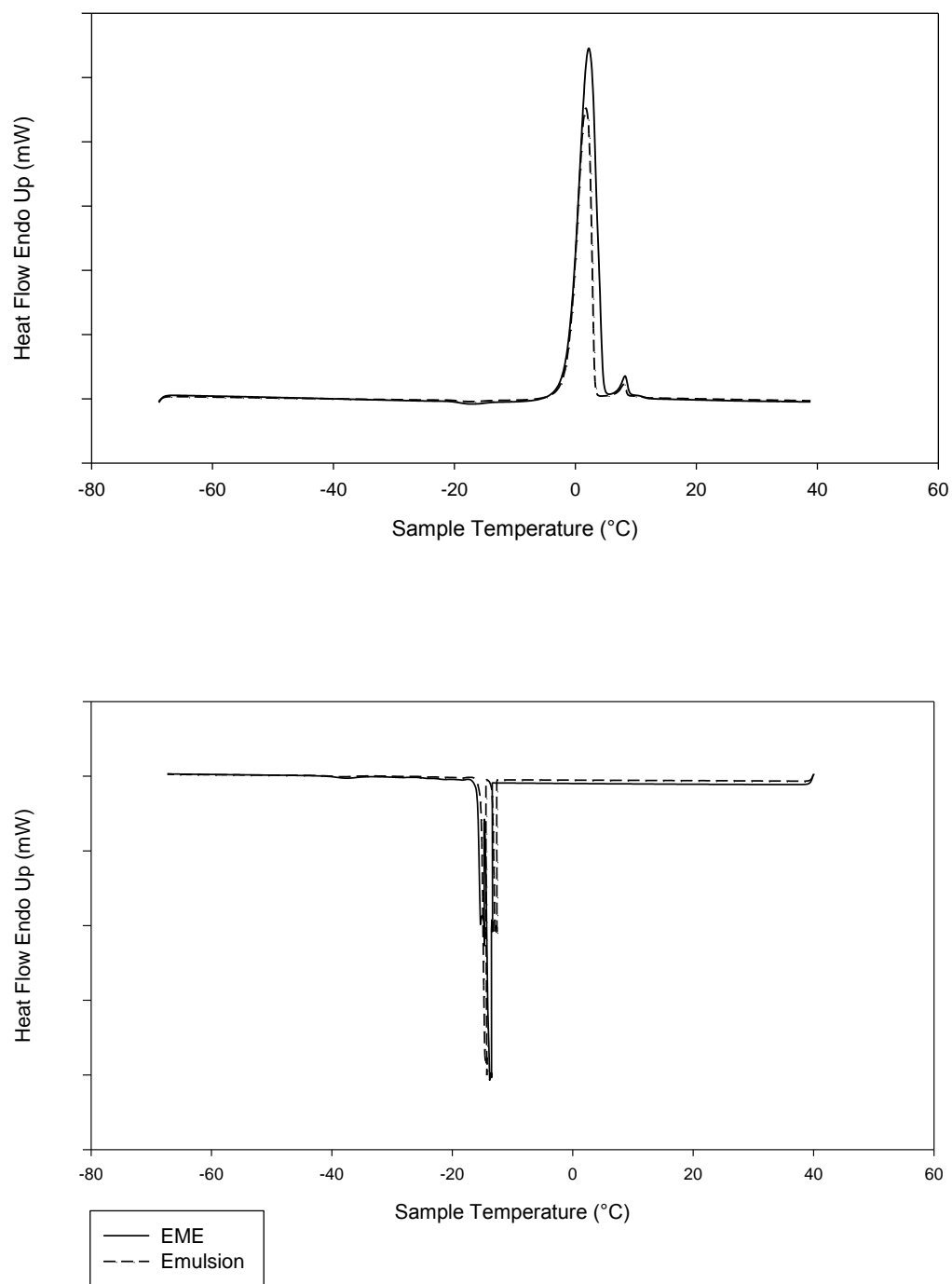


Figure 10 - Thermograms of 20% EME and 20% o/w blank emulsion, Top: Heating, Bottom: Cooling

2.8. SMALL ANGLE X-RAY SCATTERING

Structural similarity between the emulsions and the dispersed phases was examined by SAXS. The scattering profiles of the dispersed phases (ME or neat GMO:TC) were compared to that of the corresponding emulsions. The SAXS diffractograms of the EME, blank emulsion and non-dispersed bulk phases are shown in Figure 11. As the aqueous content within the ME dispersion was low, the EME samples were not diluted to maximize the scattering caused by the fine water droplets. The microemulsions were consequently undiluted when submitted to SAXS to maintain consistency with the corresponding EME.

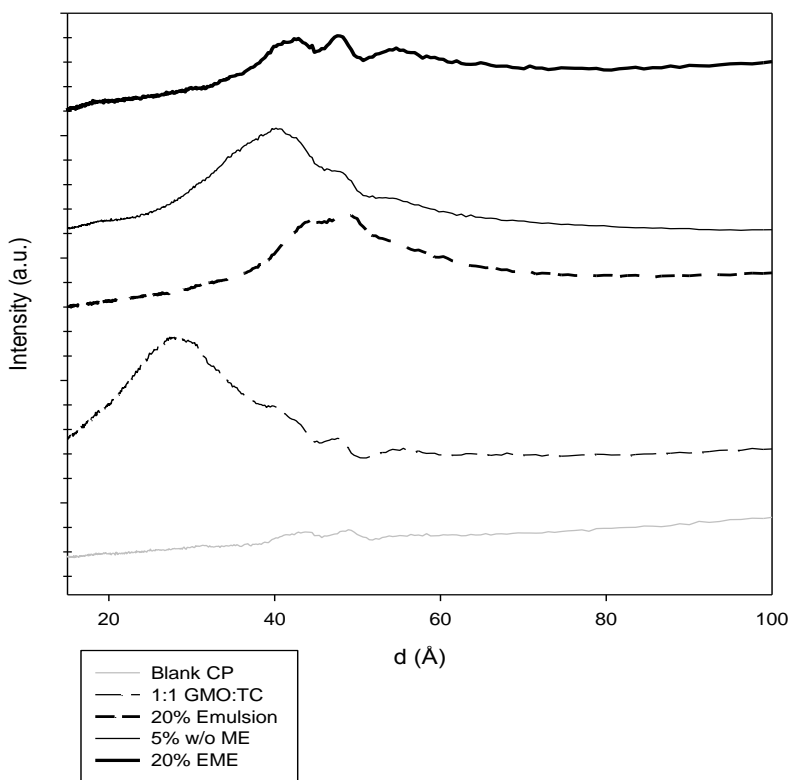


Figure 11 - Small angle x-ray scattering of 20% EME, 20% blank emulsion, and the non-dispersed microemulsion and 1:1 GMO:TC

The 5% w/o microemulsion peak displayed very intense scattering, requiring that the measured intensities for this sample to be decreased 4 times for direct comparison with the others. The remaining scattering curves were unaltered. The main peak of the EME was measured at $41.8 \pm 0.9 \text{ \AA}$. The 5% microemulsion peak occurred at $40.5 \pm 0.7 \text{ \AA}$. The blank emulsion peak was very broad and was observed at $50.1 \pm 0.6 \text{ \AA}$.

By comparing the weak scattering peaks exhibited by the continuous phase (1:3 NaCas-Pectin), it was possible to establish structural features associated with emulsification. The continuous phase gave two low intensity peaks at 43 \AA and 49 \AA . The 49 \AA peak was conserved in the EME and emulsion scattering curves. Since there was no change in peak location, it may be argued that this peak was caused by pectin. Since pectin is believed to form concentric layers around surfactant covered droplets, the scattering peak at 49 \AA may have been due to either caseinate-pectin or pectin-pectin interactions. It is also possible that the scattering was caused by the increased ordering around the casein-covered oil droplet. In whey protein-gum arabic mixtures (not emulsions), a similarly-conserved peak was determined to be a protein structure factor consistent with a hard sphere model (Weinbreck, Tromp, & de Kruif, 2004). In the case of the NaCas-Pectin system used here, it is probable that this peak was due to the formation of pectin “rings” around the large droplets.

The average d value of the main scattering peak of the 5% microemulsion at 41 \AA , the peak at 43 \AA of the continuous phase and the 42 \AA peak of the 20% EME were statistically similar ($p > 0.05$), implying no loss of microemulsion structure after emulsification. However, this did not account for the peak at 55 \AA in the EME diffractogram that was not present in the emulsion scattering or continuous phase data. Theoretically, the characteristic distance (d) value observed for the ME should persist after emulsification into an EME. However, if microemulsion droplets were lost after emulsification, it is possible that the d value would have increased as the ME droplets became less “compact”. This would account for a peak at higher values of d . It is possible

that the peak at 42 Å for the EME was not due to microemulsion structure, but to the protein-oil or protein-pectin interactions after emulsification. This is further evidenced by the broad emulsion peak at ~50 Å, which displayed some degree of scattering at ~42 Å. The true nature of this 42 Å peak was not known from this data, but could be better understood with further analysis on the NaCas-Pectin complex.

Overall, the data suggested that there was some loss of microemulsion droplets after emulsification, but that an ME dispersion was nevertheless present. These results differ from previous studies, but do indicate that this emulsification method may have affected the internal microemulsion structure.

2.9. EME CRYO-TEM

Cryo-TEM imaging of the diluted EME (Figure 12, left) shows an oil droplet suspended within an ice matrix. The striated appearance of the continuous phase was due to unvitrified water and was not attributed to sample contamination. Figure 12 (right) shows details at the oil-water interface, notably the presence of water droplets within the oil droplet.

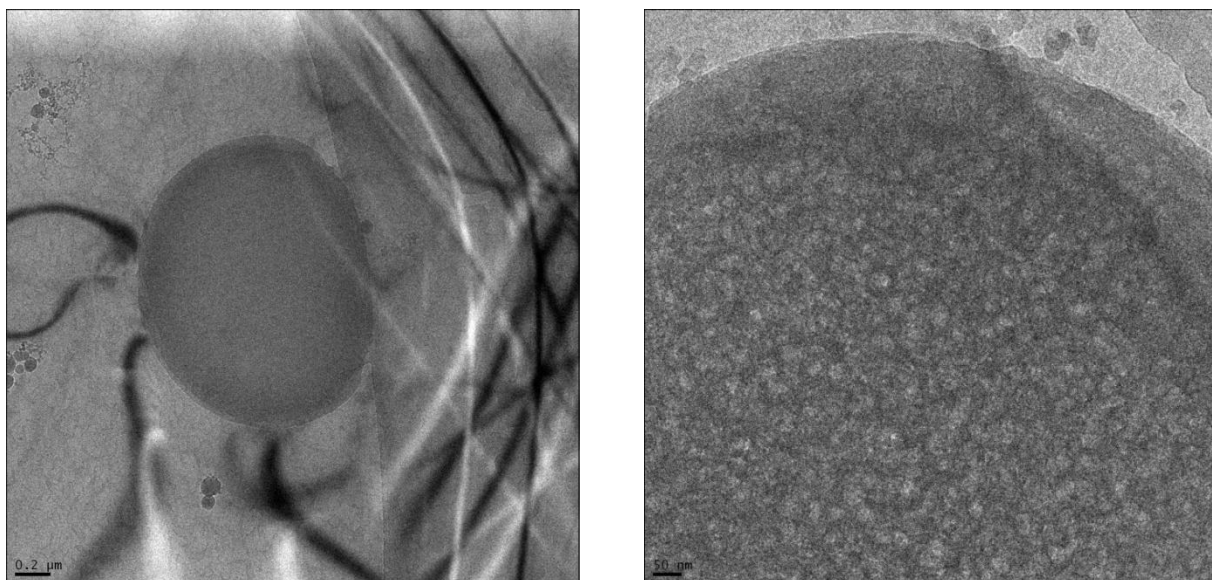


Figure 12 - Cryo-TEM of an EME droplet in partially vitrified ice, Left: Single EME droplet. Right: Close magnification of EME droplet interface showing internal structure. Light areas within droplet correspond to microemulsion dispersed aqueous domains.

These images confirmed that after emulsification, there was little or no microemulsion structure loss. This image was taken slightly out of focus as this improved the contrast between the small water droplets and the oil phase. This approach has been the basis of high-resolution cryo-TEM, which exploits the secondary phase interference produced by under-focusing objective lenses (Ayache *et al.*, 2010). There was no crystalline appearance in the inner aqueous microemulsion domains. Though the out-of-focus image provided less information in terms of resolution of the interface, it gave better detail of the internal structure of the droplet closer to the core. Additional phase contrast was provided by defocusing the image, where a secondary interference plane was produced (Ayache *et al.*, 2010; Rangelov, Momekova, & Almgren, 2010). This increased detail in internal structure is modest considering the thickness of the sample film; however, Figure 12 successfully showed droplets of under 50 nm, similar to that seen in the Cryo-TEM image of the microemulsion (Figure 6) before dispersion into aqueous sodium caseinate-pectin.

3.6. RELEASE BEHAVIOUR

In an attempt to compare this EME system with that of Pilman *et al.* (Pilman *et al.*, 1980), methylene blue was used as a water-soluble marker to monitor release and encapsulation efficiency. Release of methylene blue (Figure 13) was performed over 48 hours with 3 mL samples of the release medium extracted after 1, 2, 3, 4, 20, 24, 44 and 48 hrs in triplicate. UV absorbance of each sample was measured and converted to methylene blue concentration (ppm) through a standard curve. The percentage of methylene blue released was calculated as: $\% = 100 \times \frac{M}{M_0}$ where M = methylene blue concentration at time (t , ppm) and M_0 = total mg methylene blue in encapsulation matrix/1L release medium (ppm). This assumed 100% release of encapsulated methylene blue. Once sealed, the enclosed matrices were held in a hypotonic solution to maximize the osmotic gradient between the encapsulation matrix and the release medium.

Release of aqueous methylene blue as a control showed diffusion in the absence of an encapsulation matrix, with 95 % of the dye released within 20 hrs, primarily within the first hour. The microemulsion encapsulation of methylene blue was effective at retaining the dye, releasing only 21.7 ± 4.5 % of the dye after 48 hrs in the releasing medium. The highest rate of release after encapsulation was also within the first hour, but drastically reduced to a nearly steady state after two hours. In fact, this steady rate of release was maintained well after 48 hours, with the majority of the dye (> 75 %) still encapsulated within the microemulsion after 10 days under release conditions. Since the microemulsion was largely oil, the diffusion of encapsulated aqueous material was expected to be quite slow. Release of methylene blue from the microemulsion was expected to occur through Ostwald ripening, where the internal droplets 'carried' the compound to the bulk water phase, as seen in DE-based encapsulation matrices (Ficheux *et al.*, 1998;Garti & Benichou, 2004). Phase inversion within the sealed compartment was not observed as the oil phase showed no signs of deterioration or change in optical transparency. The microemulsion formulated in this

study was effective in the slow release of encapsulated compound and may be suitable as a controlled release vehicle without dispersion into an EME.

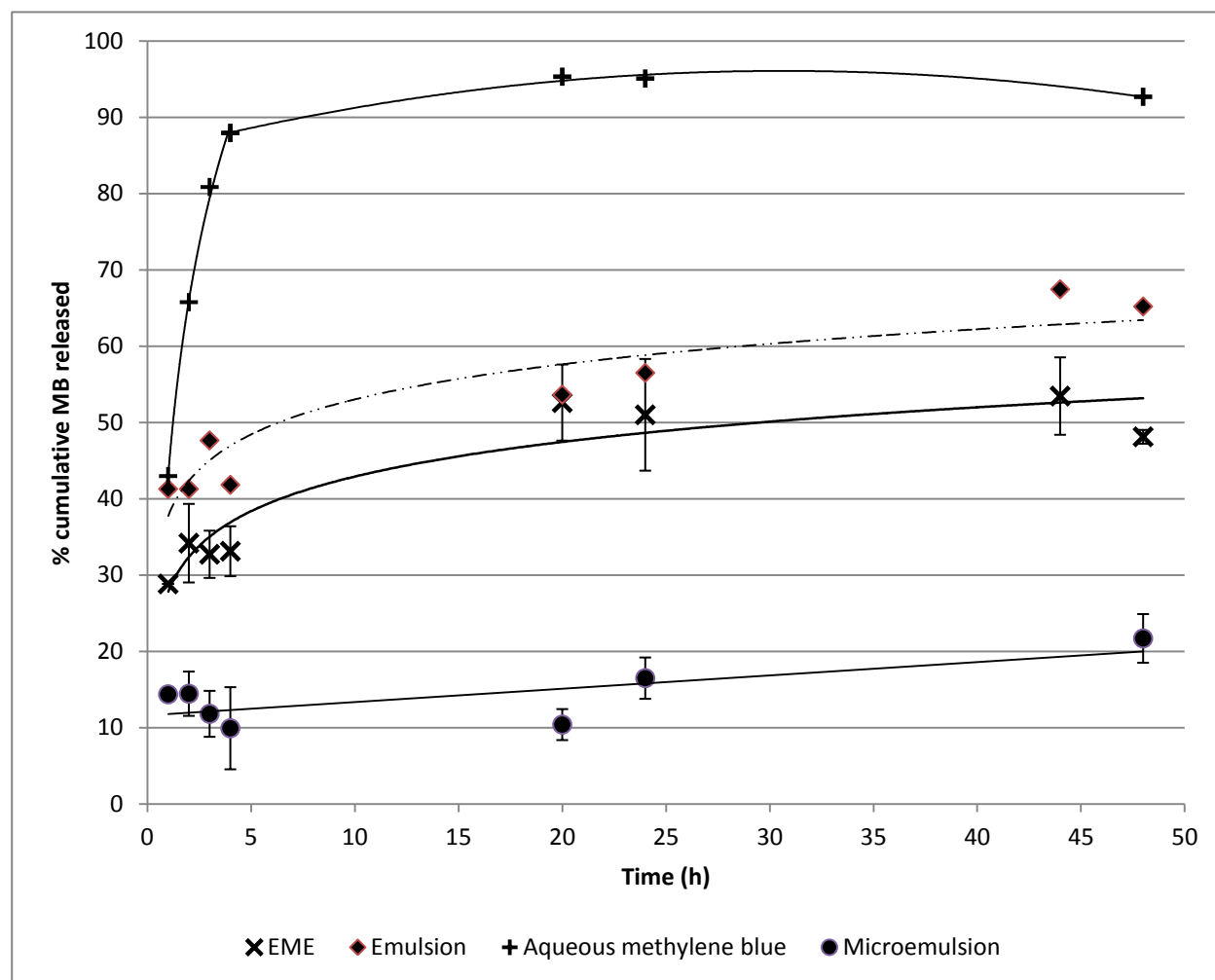


Figure 13- 48 hour release profiles of methylene blue in various matrices (EME, Emulsion, ME, aqueous).

Once the microemulsion was dispersed into the EME, encapsulation efficiency decreased, releasing approximately 50% of the solubilised dye after 24 hrs. The MBEME reached a plateau between the 20 and 48 hrs sampling intervals. The average cumulative methylene blue released during this period was $51.3 \pm 2.3\%$. The MBE had a significantly and consistently higher cumulative

average methylene blue release of $60.7 \pm 6.7\%$ between the 20 and 48 hr interval, 9.4% greater than that of the MBEME.

The sealed tubing containing emulsified samples expanded considerably during release studies due to water ingress, eventually causing EME destabilization through creaming within the sealed compartment.

The mode of release was likely reverse micellar transport, as seen in DEs (Ficheux *et al.*, 1998; Kanouni *et al.*, 2002; Matsumoto, Kita, & Yonezawa, 1976). Theoretically, the microemulsion used for this experiment should have retained high concentrations of methylene blue. However, there was the possibility that the overall emulsion was not optimized in terms of caseinate concentration. If there was too high a concentration of aqueous surfactant, casein molecules may have locally aggregated leaving interfacial areas exposed (Ficheux *et al.*, 1998; Garti & Benichou, 2004), allowing for the encapsulated species to escape into the aqueous continuous phase. If the w/o microemulsion was exposed to water without the presence of a stabilizer, osmotic pressure may have caused the release of the compound as seen in DEs. This was likely indicative that the casein concentration used in this study did not negatively affect EME stability, but did reduce encapsulation potential. To test this hypothesis, varying casein content in EMEs may establish whether casein concentration is a factor in sub-optimal release. This should be paired with microscopy studies to determine whether there is concurrent coalescence of the internal droplets, if any, over time.

The suitability of methylene blue for a casein-stabilized $w_1/o/w_2$ DE was studied by O'Regan and Mulvihill (Regan & Mulvihill, 2009). Since casein and methylene blue have opposing charges, a possible interaction may ensue after release of the encapsulated dye. This may cause low recovery in the release medium and a high degree of variability. A similarly encapsulated water-soluble marker, Vitamin B₁₂, showed improved recovery after release. In the case of the EME studied here, pectin was likely to interact with methylene blue since it has an overall negative

charge at pH ~5.5. This was shown to be the case as the blank emulsion was able to retain ~50% of the non-encapsulated dye when added in the continuous phase only. However, since the EME was shown to have ~9% greater encapsulation efficiency over the blank emulsion, this system successfully encapsulated the aqueous marker, showing that it was suitable as a controlled delivery system. Comparison of an uncharged marker encapsulated within the inner aqueous phase would be suitable for future studies using this system.

In comparison to the EME system described by Pilman *et al.*, the emulsion presented here had superior stability, but was not as efficient at encapsulating methylene blue. A possible reason may be the casein content, which was higher in the previously described study. There was a possible interaction between the protein and the dye, notably at pH = 7 where the protein carries negative charge. Under these conditions, the released dye may have moved into the w_2 phase through reverse micellar transport, but subsequently interacted with casein. This dye was then essentially trapped within the w_2 compartment after release. The release results using the present EME system strongly showed that the same conditions that affect DE stability clearly affected the EMEs in spite of a thermodynamically stable interior.

4. CONCLUSION

This work aimed to create a food-grade emulsified microemulsion capable of encapsulating a cationic dye. Microemulsion characterization involving DSC, Cryo-TEM and SAXS showed that the food-grade system created for this study adhered to structural criteria in terms of size domains, a disordered internal arrangement and presence of core water. The microemulsion was effective at retaining internalized methylene blue, ~ 78% after 48 hours in the releasing medium.

It is clear from the SAXS and Cryo-TEM that the internal structure of the microemulsion was maintained after emulsification. However, at 20% dispersed phase content within the EME, the

enthalpic signatures unique to an internal microemulsion were lost. EMEs capable of higher oil loading would be more appropriate for this method of characterization.

The research objectives, in terms of creating a structural profile for this complex system, were met. In terms of stability, this system was stable for up to 14 days, which was less than the desired length of stability (*i.e.* months), however, this system did exhibit improved stability over a previous food-grade system.

Release studies showed that there was a modest retention of dye after 48 hours and that the methylene blue encapsulated within the EME was more effectively retained than the blank emulsion with no encapsulated compound. Release of the encapsulated dye may have been due to excess sodium caseinate in the EME causing inadequately-covered areas of the oil droplet surface. This was attributed to Ostwald ripening, giving rise to the unintentional release of the guest compound. It was also shown that EME formulations are subject to similar destabilization processes that affect DEs. There was marked release of encapsulated methylene blue; however, this system was effective at retaining ~9% of the encapsulated compound after 48 hours.

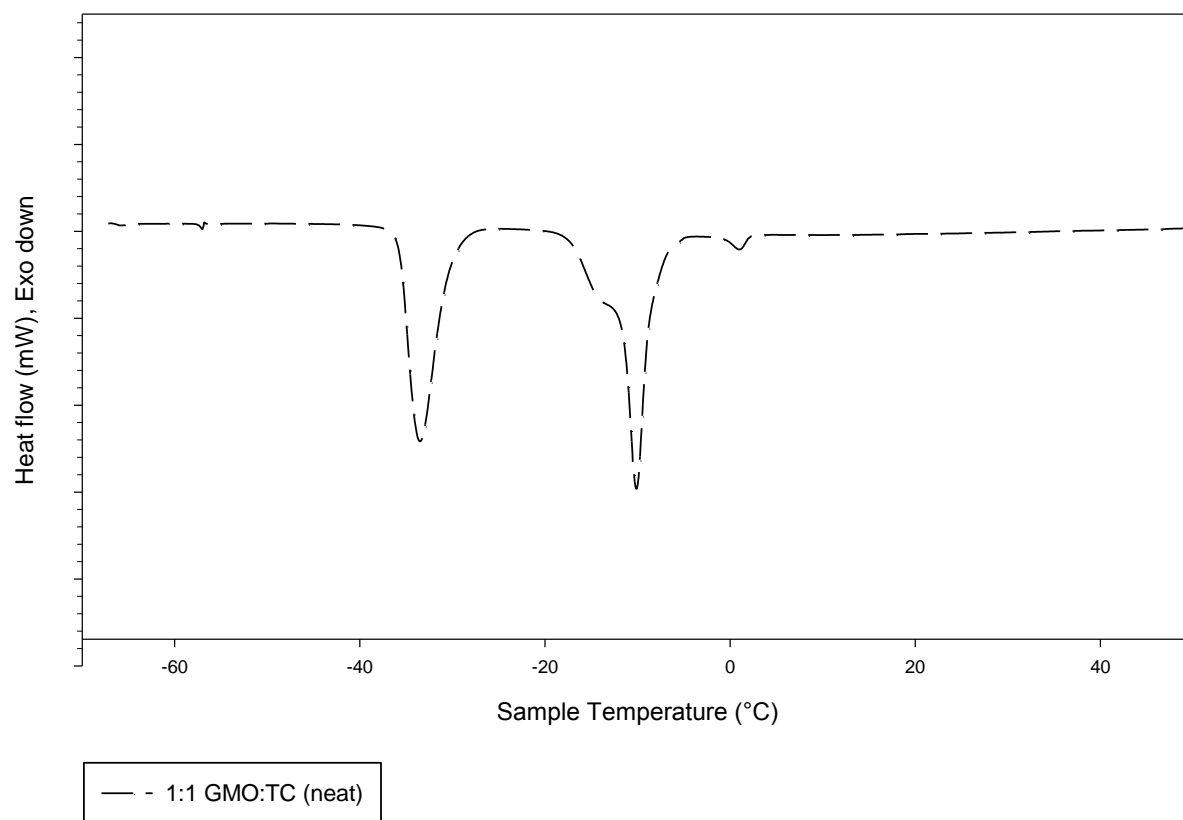
In conclusion, a food-grade ME was successfully characterized by Cryo-TEM, DSC and SAXS. Its corresponding EME produced *via* membrane emulsification displayed shelf stability for up to 14 days at room temperature. It was characterized by Cryo-TEM and SAXS and showed that the internal dispersion was retained after emulsification. Functional studies showed that the EME could encapsulate methylene blue and release it over a period of 48 hours ~9% more effectively than a non-nanostructured emulsion. Although the system described in this work requires optimization to improve release behaviour and encapsulation ability, it would be well-suited for oral administration of compounds requiring release over the span of 1 to 2 days. Some possible applications include matrices for delivering diagnostic imaging contrasts, chemotherapeutics, probiotic compounds and vitamins.

4.1. FUTURE WORK

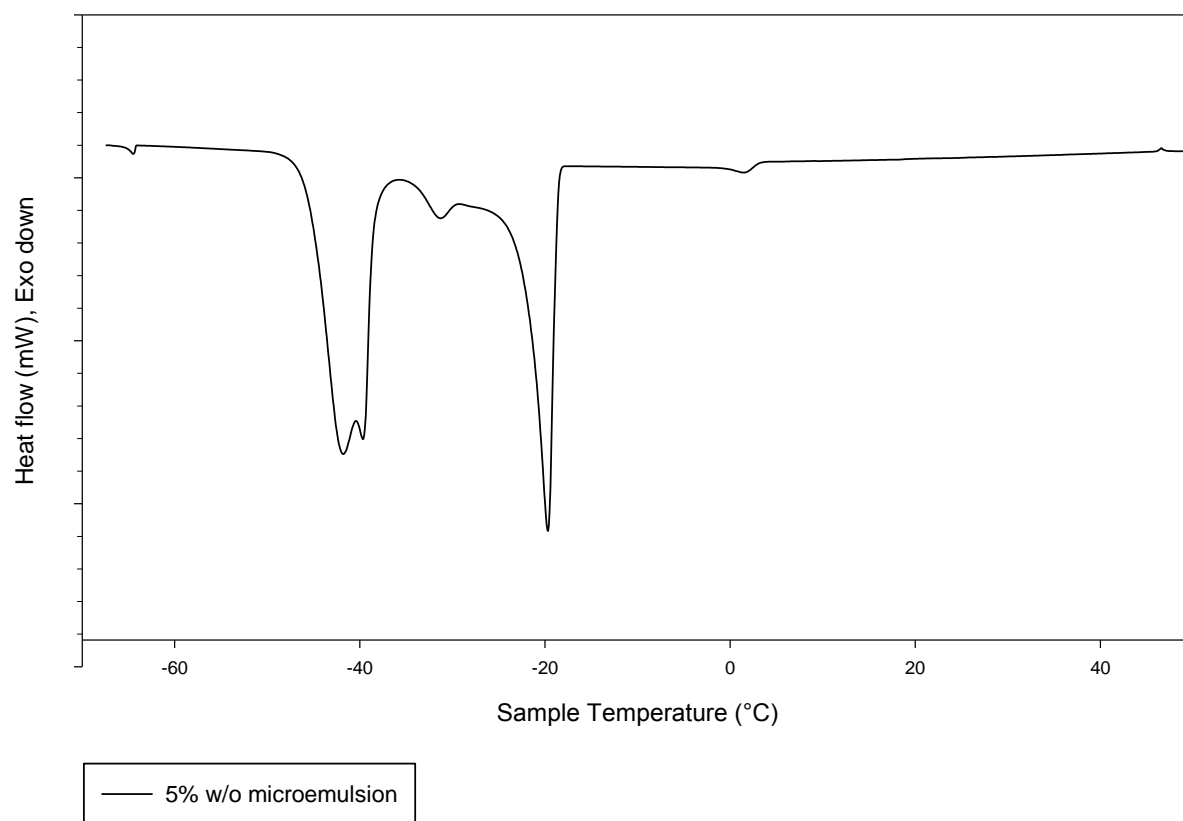
The EME system presented here holds potential for controlled release. Optimization of the EME is necessary to identify how it can be applied to various delivery matrices. Future studies using this system include:

1. Optimization of casein content. This would maximize retention time of the guest compound within the ME compartment by preventing reverse micellar transport.
2. Investigation of alternative water-soluble markers for encapsulation (*i.e.* Vitamin B₁₂, NaCl, proteins/protein catalysts, Vitamin C). This would also indicate appropriate industrial applications, such as antioxidant encapsulation, catalysis, and sustained release drug delivery.
3. Refine imaging techniques for structural studies on EME structure. One possible method is freeze-fracture Cryo-SEM.
4. Release kinetic studies to determine rate and mode of release of encapsulated compounds. This is especially relevant for optimizing the EME system for use as a drug delivery system.
5. Rheological studies to determine physical properties of the EME and how this system can be applied to food and other consumer products.

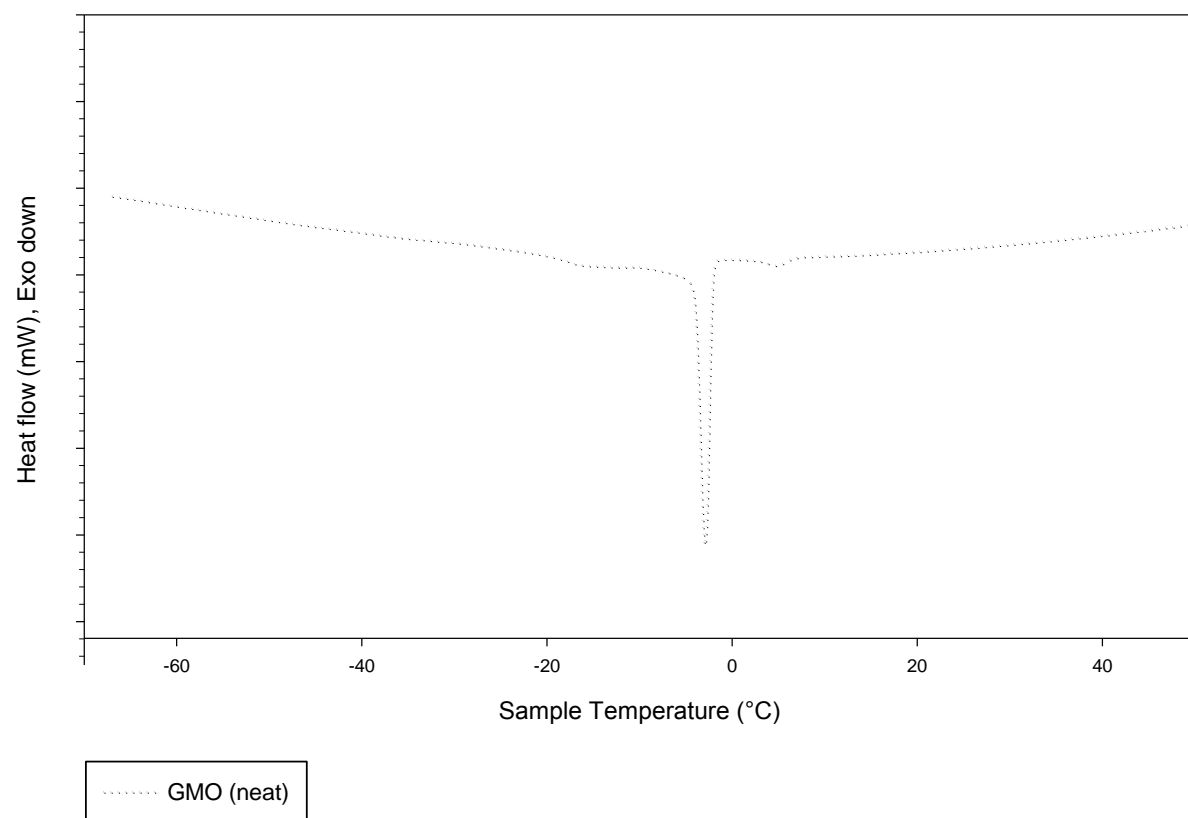
5. APPENDIX



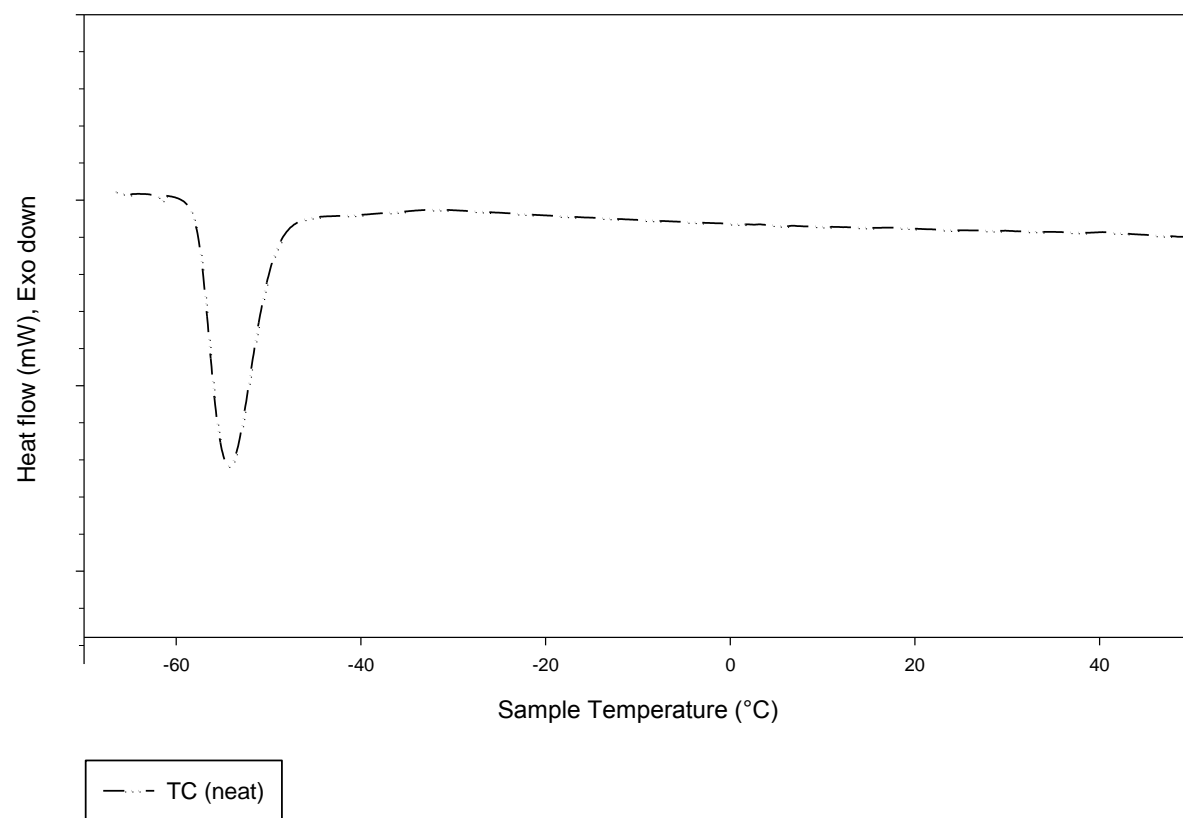
Appendix 1 - Cooling thermogram of neat 1:1 GMO:TC



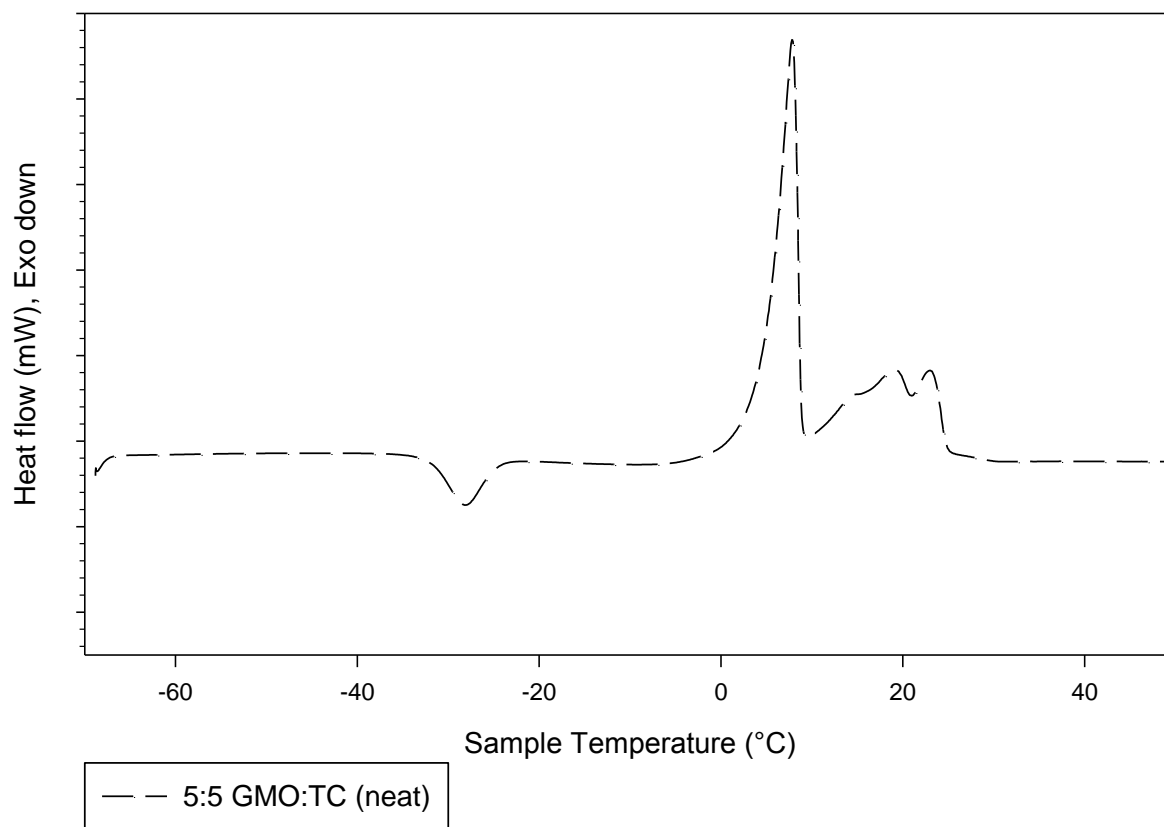
Appendix 2 - Cooling thermogram of 5% w/o microemulsion



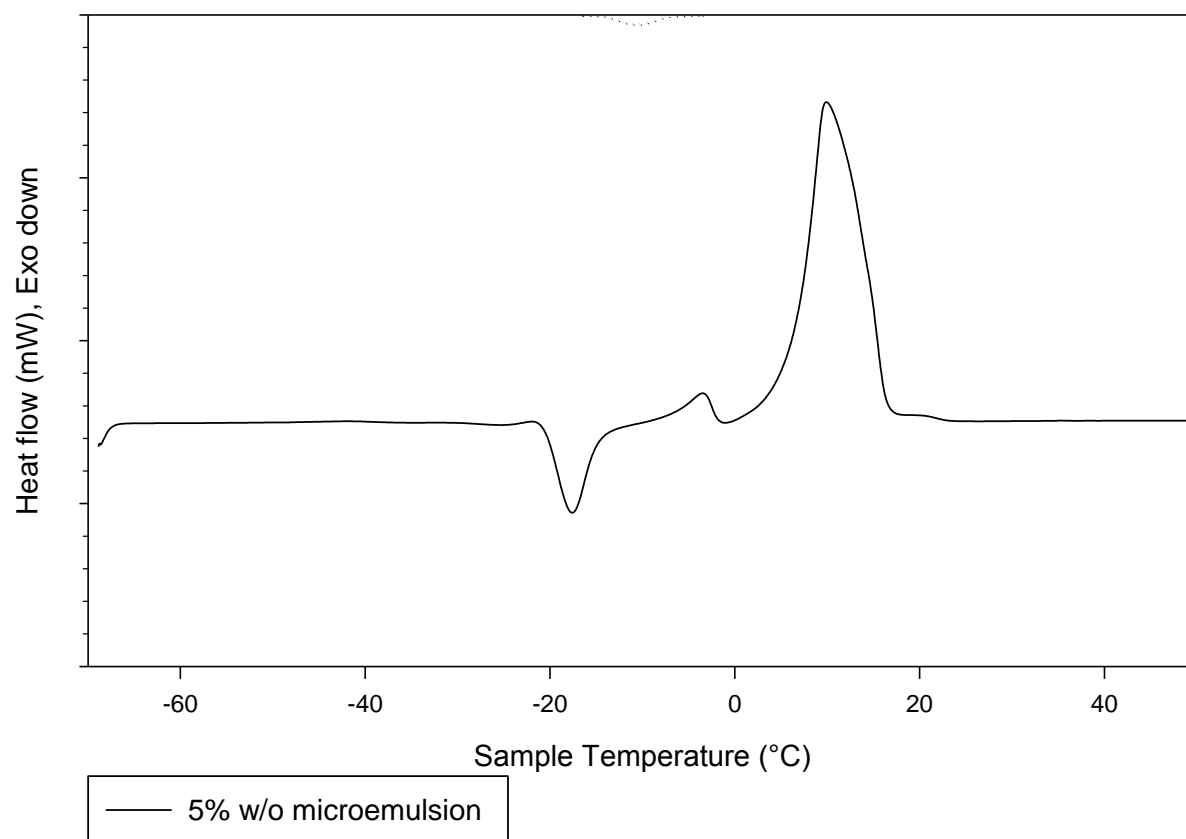
Appendix 3 - Cooling thermogram of neat GMO



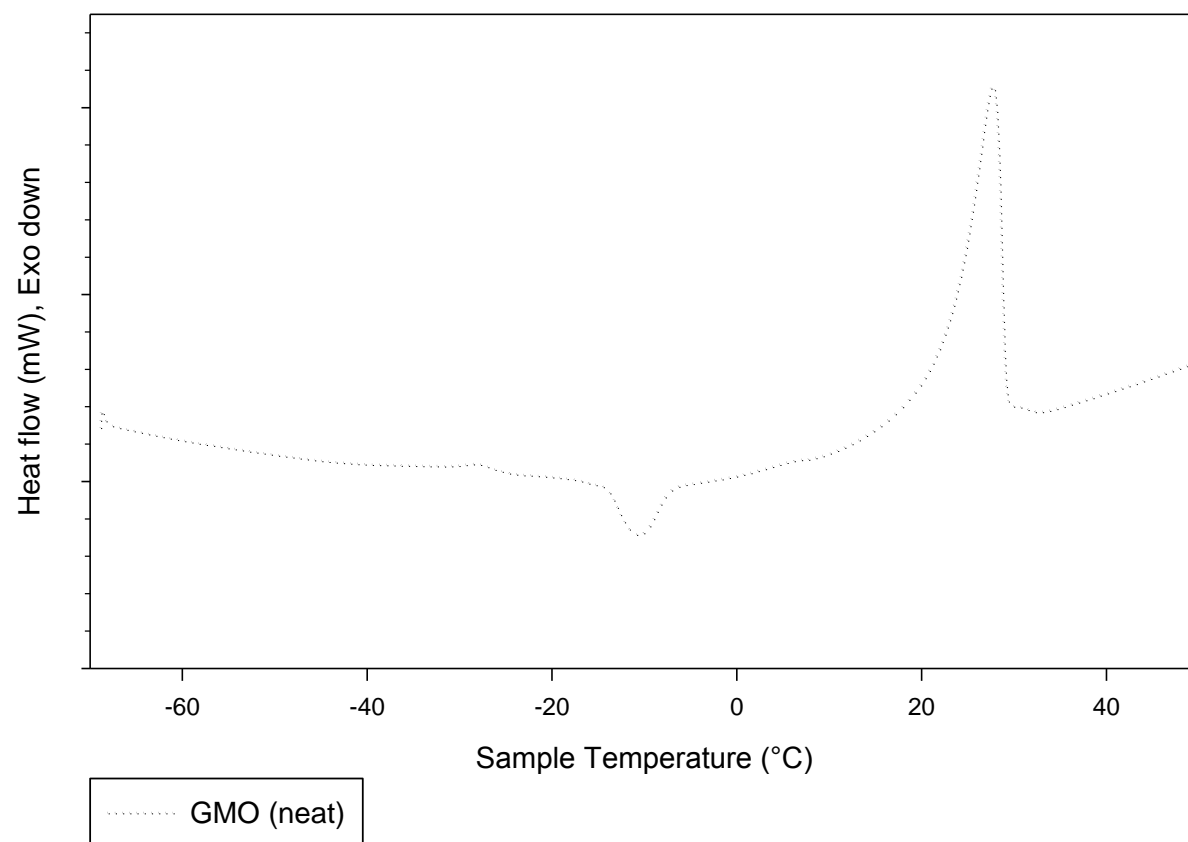
Appendix 4 - Cooling thermogram of neat TC



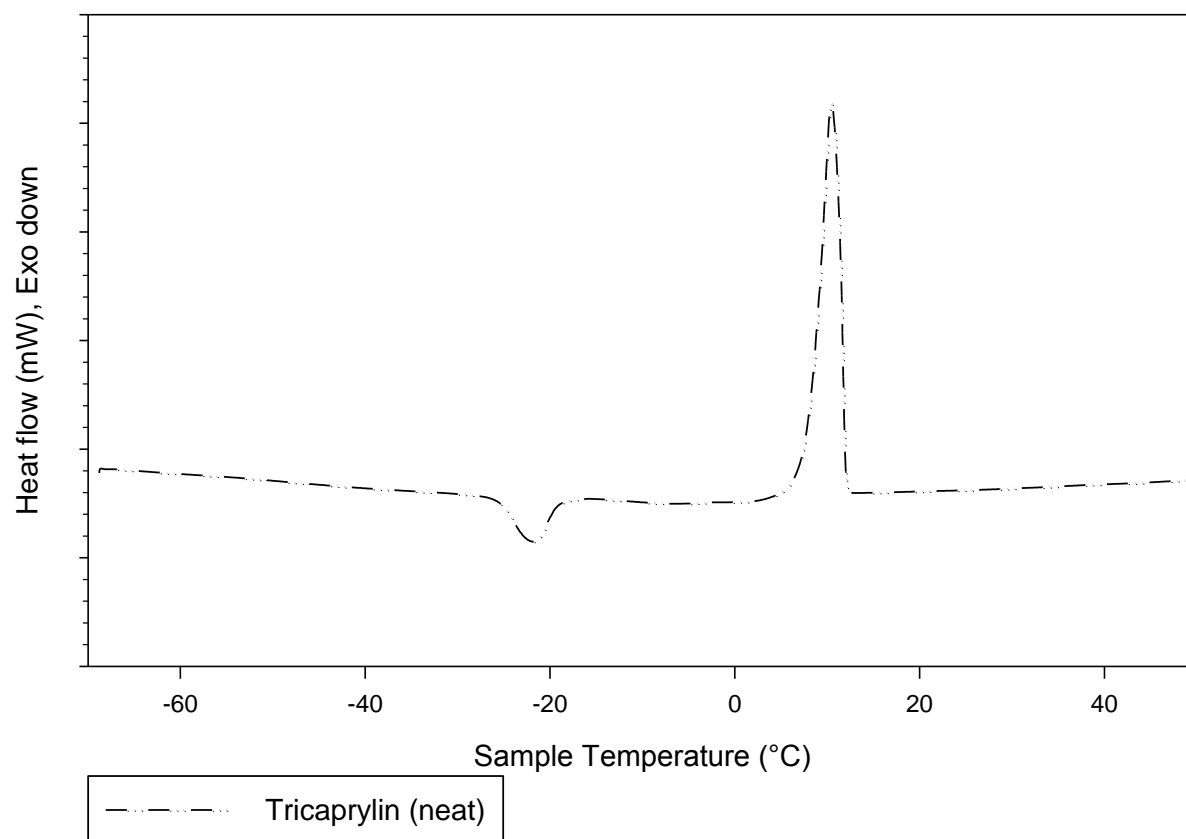
Appendix 5 - Heating Thermogram of 1:1 GMO:TC



Appendix 6 - Heating thermogram of 5% w/o microemulsion



Appendix 7 - Heating thermogram of neat GMO



Appendix 8 - Heating thermogram of neat TC

6. BIBLIOGRAPHY

- Amar-Yuli, I., & Garti, N. (2005). Transitions induced by solubilized fat into reverse hexagonal mesophases. *Colloids and surfaces B Biointerfaces*, 43(2), 72–82.
- Ayache, J., Beunier, L., Boumendil, J., Ehret, G., & Laub, D. (2010). *Sample preparation handbook for transmission electron microscopy: Methodology*. New York, NY, USA: Springer.
- Benichou, A., Aserin, A., & Garti, N. (2007a). W/O/W double emulsions stabilized with WPI–polysaccharide complexes. *Colloids and Surfaces A: Physicochemical and Engineering Aspects*, 294(1-3), 20–32.
- Benichou, A., Aserin, A., & Garti, N. (2007b). O/W/O double emulsions stabilized with WPI–polysaccharide conjugates. *Colloids and Surfaces A: Physicochemical and Engineering Aspects*, 297(1-3), 211–220.
- Bonnet, C., Corredig, M., & Alexander, M. (2005). Stabilization of caseinate-covered oil droplets during acidification with high methoxyl pectin. *Journal of Agricultural and Food Chemistry*, 53(22), 8600–8606.
- Chen, J., & Dickinson, E. (1995a). Protein surfactant interfacial interactions - Part I: Flocculation of emulsions containing mixed protein and surfactant. *Colloids and Surfaces A: Physicochemical and Engineering Aspects*, 100, 155–265.
- Chen, J., & Dickinson, E. (1995b). Protein surfactant interfacial interactions - Part 2: Electrophoretic mobility of mixed protein and surfactant systems. *Colloids and Surfaces A: Physicochemical and Engineering Aspects*, 100, 267–277.
- Considine, T., Noisuwan, A., Hemar, Y., Wilkinson, B., Bronlund, J., & Kasapis, S. (2011). Rheological investigations of the interactions between starch and milk proteins in model dairy systems: A review. *Food Hydrocolloids*, 25(8), 2008–2017.
- Constantinides, P. P., & Scalart, J. P. (1997). Formulation and physical characterization of water-in-oil microemulsions containing long- versus medium- chain glycerides. *International Journal of Pharmaceutics*, 158, 57–63.
- Dalgleish, D. G. (1996). Food Emulsions. In S. Johan (Ed.), *Emulsions and Emulsion Stability* (pp. 287–325). New York, New York: Marcel Dekker Inc.
- Dalgleish, D. G. (2011). On the structural models of bovine casein micelles—review and possible improvements. *Soft Matter*, 7, 2265–2272.
- Dickinson, E. (2001). Milk protein interfacial layers and the relationship to emulsion stability and rheology. *Colloids and Surfaces. B, Biointerfaces*, 20(3), 197–210.
- Dickinson, E. (2010a). Double Emulsions Stabilized by Food Biopolymers. *Food Biophysics*, 6(1), 1–11. 56

- Dickinson, E. (2010b). Flocculation of protein-stabilized oil-in-water emulsions. *Colloids and Surfaces. B, Biointerfaces*, 81(1), 130–40.
- Dickinson, E, Evison, J., Gramshaw, J. W., & Schwöpe, D. (1994). Flavour release from a protein-stabilized water-in-oil-in-water emulsion. *Food Hydrocolloids*, 8(1), 63–67.
- Dickinson, E., Semenova, M. G., Antipova, A. S., & Pelan, E. G. (1998). Dickinson - effect of high methoxy pectin on properties of casein stabilized emulsions. *Food Hydrocolloids*, 12, 425–432.
- Engstrom, L. (1990). Aggregation and Structural Schanges in the L2-Phase in the System Water/Soybean Oil/Sunflower Oil Monoglycerides. *Journal of Dispersion Science and Technology*, 11(5), 479–489.
- Ezrahi, S, Nir, I., Aserin, A., Kozlovich, N., Feldman, Y., & Garti, N. (2002). Dielectric and Calorimetric Characteristics of Bound and Free Water in Surfactant-Based Systems, 23, 351–378.
- Ezrahi, S, Tuval, E., & Aserin, a. (2006). Properties, main applications and perspectives of worm micelles. *Advances in colloid and interface science*, 128-130(2006), 77–102.
- Ezrahi, S., Aserin, A., Fanun, M., & Garti, N. (2000). Sub-zero Temperature Behaviour of Water in Microemulsions. In Nissim Garti (Ed.), *Thermal Behaviour of Dispersied Systems* (pp. 59–120). New York, New York: Marcel Dekker Inc.
- Fanun, M. (2009a). Microstructure of Mixed Nonionic Surfactants Microemulsions Studied By SAXS and DLS. *Journal of Dispersion Science and Technology*, 30(1), 115–123.
- Fanun, M. (2009b). Properties of microemulsions based on mixed nonionic surfactants and mixed oils. *Journal of Molecular Liquids*, 150(1-3), 25–32.
- Feigin, L. A., & Svergun, D. I. (1987). *Structure Analysis by Small Angle X-ray and Neutron Scattering..* New York, New York: Plenum Press.
- Ficheux, M., Bonakdar, L., & Bibette, J. (1998). Some Stability Criteria for Double Emulsions. *Langmuir*, 7463(11), 2702–2706.
- Frasch-Melnik, S., Norton, I. T., & Spyropoulos, F. (2010). Fat-crystal stabilised w/o emulsions for controlled salt release. *Journal of Food Engineering*, 98(4), 437–442.
- Friberg, S. E. (1985). Microemulsions. *Journal of Dispersion Science and Technology*, 6(3), 317–337.
- Gallarate, M., Carlotti, M. E., Trotta, M., & Ugazio, E. (2004). Disperse systems as topical formulations containing alpha-tocopherol. *Journal of Drug Delivery Science and Technology*, 14(6), 471–477.
- Gao, Z., Choi, H.-G., Shin, H.-J., Park, K.-M., Lim, S.-Je., Hwang, K.-J., & Kim, C.-K. (1998). Physicochemical characterization and evaluation of a microemulsion system for oral delivery of cyclosporin A. *International journal of pharmaceutics*, 161, 75–86.

- Garti, N., Aserin, A., Tiunova, I., & Fanun, M. (2000). A DSC study of water behavior in water-in-oil microemulsions stabilized by sucrose esters and butanol. *Colloids and Surfaces A: Physicochemical and Engineering Aspects*, 170, 1–18.
- Garti, N., Yaghmur, A., Leser, M. E., Clement, V., & Watzke, H. J. (2001). Improved oil solubilization in oil/water food grade microemulsions in the presence of polyols and ethanol. *Journal of Agricultural and Food Chemistry*, 49(5), 2552–2562.
- Garti, N., & Benichou, A. (2004). Recent Developments in Double Emulsions for Food Applications. In S. E. Friberg, K. Larsson, & J. Sjoblom (Eds.), *Food Emulsions* (4th ed., pp. 353–412). Marcel Decker.
- Garti, N., & Yuli-Amar, I. (2008). Micro- and Nano-emulsions for Delivery of Functional Food Ingredients. In Nissim Garti (Ed.), *Delivery and Controlled Release of Bioactives in Foods and Nutraceuticals* (pp. 149–183). Woodhead Publishing in Food Science.
- Guillot, S., Moitzi, C., Salentinig, S., Sagalowicz, L., Leser, M. E., & Glatter, O. (2006a). Direct and indirect thermal transitions from hexosomes to emulsified micro-emulsions in oil-loaded monoglyceride-based particles. *Colloids and Surfaces A: Physicochemical and Engineering Aspects*, 291(1-3).
- Guillot, S., Moitzi, C., Salentinig, S., Sagalowicz, L., Leser, M. E., & Glatter, O. (2006b). Direct and indirect thermal transitions from hexosomes to emulsified micro-emulsions in oil-loaded monoglyceride-based particles. *Colloids and Surfaces A: Physicochemical and Engineering Aspects*, 291(1-3), 78–84.
- Gustafsson, J., Ljusberg-Wahren, H., Almgren, M., & Larsson, K. (1997). Submicron Particles of Reversed Lipid Phases in Water Stabilized by a Nonionic Amphiphilic Polymer. *Langmuir*, 13(26), 6964–6971.
- Hanaor, D., Michelazzi, M., Leonelli, C., & Sorrell, C. C. (2012). The effects of carboxylic acids on the aqueous dispersion and electrophoretic deposition of ZrO₂. *Journal of the European Ceramic Society*, 32(1), 235–244.
- Higashi, S., Shimizu, M., Uchiyama, F., Tamura, S., & Setoguchi, T. (1995). Arterial-Injection Chemotherapy for Hepatocellular Carcinoma Using Monodispersed Poppy-Seed Oil Microdroplets Containing Fine Aqueous Vesicles of Epirubicin. *Cancer*, 75(6), 1245–1254.
- Hino, T., Kawashima, Y., & Shimabayashi, S. (2000). Basic study for stabilization of w / o / w emulsion and its application to transcatheter arterial embolization therapy. *Advanced Drug Delivery Reviews*, 45, 27–45.
- Joscelyne, S. M., & Trägårdh, G. (2000). Membrane emulsification — a literature review. *Journal of Membrane Science*, 169, 107–117.
- Jourdain, L., Leser, M. E., Schmitt, C., Michel, M., & Dickinson, E. (2008). Stability of emulsions containing sodium caseinate and dextran sulfate: Relationship to complexation in solution. *Food Hydrocolloids*, 22(4), 647–659. 58

- Kanouni, M., Rosano, H. L., & Naouli, N. (2002). Preparation of a stable double emulsion (W1/O/W2): role of the interfacial films on the stability of the system. *Advances in Colloid and Interface Science*, 99(3), 229–54.
- Koch, M. H. . (2006). X-ray Scattering of Non-Crystalline Biological systems using synchrotron radiation. *Chemical Society Reviews*, 35, 123–133.
- Kulkarni, C. V., Mezzenga, R., & Glatter, O. (2010). Water-in-oil nanostructured emulsions: towards the structural hierarchy of liquid crystalline materials. *Soft Matter*, 6(21), 5615.
- Kunieda, H., & Shinoda, K. (1985). Evaluation of the Hydrophile-Lipophile Balance (HLB) of Nonionic Surfactants. *Journal of Colloid and Interface Science*, 107(1), 107-121.
- Langevin, D. (1988). Microemulsions. *Accounts of Chemical Research*, 2(7), 255–260.
- Langevin, D. (1992). Micelles and Microemulsions. *Annual Review of Physical Chemistry*, 43, 341–369.
- Larsson, K. (1991). *Emulsions of Reversed Micellar Phases and Aqueous Dispersions of Cubic Phases of Lipids*. (M. El-Nokaly & D. G. Cornell, Eds.) *Microemulsions and Emulsions in Foods* (pp. 44–50). American Chemical Society.
- Lawrence, M. J., & Rees, G. D. (2000). Microemulsion-based media as novel drug delivery systems. *Advanced Drug Delivery Reviews*, 45, 89–121.
- Leal-Calderon, F., Bibette, J., & Schmitt, V. (2007). *Emulsion Science: Basic Principles* (pp. 5–51). New York, New York: Springer.
- Libster, D, Aserin, a, & Garti, N. (2006). A novel dispersion method comprising a nucleating agent solubilized in a microemulsion, in polymeric matrix II. Microemulsion characterization. *Journal of Colloid and Interface Science*, 302(1), 322–9.
- Libster, D., Aserin, A., Yariv, D., Shoham, G., & Garti, N. (2009). Soft matter dispersions with ordered inner structures, stabilized by ethoxylated phytosterols. *Colloids and Surfaces. B, Biointerfaces*, 74(1), 202–15.
- Lopes da Silva, J. A., & Rao, M. A. (2006). Pectins: Structure, Functionality, and Uses. In A. M. Stephen, G. O. Phillips, & P. A. Williams (Eds.), *Food Polysaccharides and Their Applications* (pp. 353–411). Boca Raton: CRC Press.
- Lutz, R., Aserin, A., Wachtel, E. J., Ben-Shoshan, E., Danino, D., & Garti, N. (2007). A Study of the Emulsified Microemulsion by SAXS, Cryo-TEM, SD-NMR, and Electrical Conductivity. *Journal of Dispersion Science and Technology*, 28(8), 1149–1157.
- Lutz, R., Aserin, A., Wicker, L., & Garti, N. (2009). Release of electrolytes from W/O/W double emulsions stabilized by a soluble complex of modified pectin and whey protein isolate. *Colloids and Surfaces. B, Biointerfaces*, 74(1), 178–85. 59

- Matsumoto, S., Kita, Y., & Yonezawa, D. (1976a). An attempt at preparing water-in-oil-in-water multiple phase emulsions. *Journal of Colloid and Interface Science*, 57(2), 353-361.
- McClements, D. J. (2012). Nanoemulsions versus microemulsions: terminology, differences, and similarities. *Soft Matter*, 8(6), 1719.
- Morais, J. M., Santos, O. D. H., Nunes, J. R. L., Zanatta, C. F., & Rocha-Filho, P. a. (2008). W/O/W Multiple Emulsions Obtained by One-Step Emulsification Method and Evaluation of the Involved Variables. *Journal of Dispersion Science and Technology*, 29(1), 63-69.
- Mueller, E., Kovarik, J. M., van Bree, J. B., Tetzloff, W., Grevel, J., & Kutz, K. (1994). Improved dose linearity of cyclosporine pharmacokinetics from a microemulsion formulation *Pharmaceutical Research*, 11(2), 301-304.
- Nakashima, T., Shimizu, M., & Kukizaki, M. (2000). Particle control of emulsion by membrane emulsification and its applications. *Advanced Drug Delivery Reviews*, 45, 47-56.
- Narang, A. S., Delmarre, D., & Gao, D. (2007). Stable drug encapsulation in micelles and microemulsions. *International Journal of Pharmaceutics*, 345(1-2), 9-25.
- Parris, N., Joubran, R. F., & Lu, D. P. (1994). Triglyceride Microemulsions : Effect of Nonionic Surfactants and the Nature of the Oil. *Journal of Agricultural and Food Chemistry*, 42, 1295-1299.
- Pays, K., Giermanska-Kahn, J., Pouligny, B., Bibette, J., & Leal-Calderon, F. (2002). Double emulsions : how does release occur? *Journal of Controlled Release*, 79, 193-205.
- Pilman, E., Karsson, K., & Tornberg, E. (1980). Inverse Micellar Phases in Ternary Systems of Polar Lipids/Fat/Water and Protein Emulsification of Such Phases to W/O/W-Microemulsion-Emulsions. *Dispersion Science and Technology*, 1(3), 267-281.
- Pilman, E., Tornberg, E., & Larsson, K. (1982). Interfacial Tension Between an Inverse Micellar Phase of Lipid Components and Aqueous Protein Solutions. *Journal of Dispersion Science and Technology*, 3(3), 335-349.
- Quemada, D., & Langevin, D. (1985). Rheological modelling of microemulsions. *Journal of Theoretical and Applied Mechanics*, Special Issue, 201-237.
- Rakshit, A. K., & Moulik, S. P. (2009). Physicochemistry of W/O Microemulsions: Formation, Stability and Droplet Clustering. In M. Fanun (Ed.), *Microemulsions: Properties and Applications* (pp. 17-57). Boca Raton: CRC Press.
- Rangelov, S., Momekova, D., & Almgren, M. (2010). Structural characterization of lipid-based colloidal dispersions using cryogenic transmission electron microscopy. *Microscopy: Science, Technology, Applications and Education*, 1724-1734. 60

- Regan, J. O., & Mulvihill, D. M. (2009). Water soluble inner aqueous phase markers as indicators of the encapsulation properties of water-in-oil-in-water emulsions stabilized with sodium caseinate. *Food Hydrocolloids*, 23(8), 2339–2345.
- Rosano, H. L., Gandolfo, G., & Hidrot, J. P. (1998). Stability of W1/O/W2 multiple emulsions Influence of ripening and interfacial interactions. *Colloids and Surfaces A: Physicochemical and Engineering Aspects*, 138, 109–121.
- Rosen, M. J., & Kunjappu, J. T. (2012). *Surfactants and Interfacial Phenomena* (4th ed., pp. 1–6, 336–367). Hoboken, New Jersey: Wiley.
- Rozman, B., & Gasperlin, M. (2007). Stability of vitamins C and E in topical microemulsions for combined antioxidant therapy. *Drug delivery*, 14(4), 235–45.
- Ruckenstein, E., & Chi, J. C. (1974). Stability of Microemulsions. *Journal of the Chemical Society: Faraday Transactions 2: Molecular and Physical Dynamics*, 71, 1690–1707.
- Sagalowicz, L., Michel, M., Adrian, M., Frossard, P., Rouvet, M., Watzke, H. J., Leser, M. E. (2006). Crystallography of Dispersed Liquid Crystalline Phases Studies by Cryo-Transmission Electron Microscopy. *Journal of Microscopy*, 221(2), 110–121.
- Salonen, A., & Glatter, O. (2010). Internally Self-Assembled Submicrometer Emulsions Stabilized by Spherical Nanocolloids : Finding the Free Nanoparticles in the Aqueous Continuous Phase, 26(27), 9512–9518.
- Schulz, P. C. (1998). DSC analysis of the state of water in surfactant-based microstructures. *Journal of Thermal Analysis*, 51, 135–149.
- Senatra, D. (2000). Thermal Analysis of Self-Assembling Complex Liquids. In Nissim Garti (Ed.), *Thermal Behaviour of Dispersed Systems* (pp. 203–245). Boca Raton: Marcel Dekker Inc.
- Shinoda, K., & Saito, H. (1968). The Effect of Temperature on the Phase Equilibria and the Types of Dispersions of the Ternary System Composed of Water, Cyclohexane, and nonionic Surfactant. *Journal of Colloid and Interface Science*, 26, 70–74.
- Spernath, A., & Aserin, A. (2006). Microemulsions as carriers for drugs and nutraceuticals. *Advances in Colloid and Interface Science*, 128-130(2006), 47–64.
- Teubner, M., & Strey, R. (1987). Origin of the scattering peak in microemulsions. *The Journal of Chemical Physics*, 87(5), 3195.
- Tuinier, R., Rolin, C., & de Kruif, C. G. (2002). Electrosorption of pectin onto casein micelles. *Biomacromolecules*, 3(3), 632–8.
- Villa, C. H., Lawson, L. B., Li, Y., & Papadopoulos, K. D. (2003). Internal Coalescence as a Mechanism of Instability in Water-in-Oil-in-Water Double-Emulsion Globules. *Langmuir*, (13), 244–249. 61.

- Vrignaud, S., Anton, N., Gayet, P., Benoit, J., & Saulnier, P. (2011). Reverse micelle-loaded lipid nanocarriers : A novel drug delivery system for the sustained release of doxorubicin hydrochloride. *European Journal of Pharmaceutics and Biopharmaceutics*, 79(1), 197–204.
- Weinbreck, F., Tromp, R., & de Kruif, C. G. (2004). Composition and structure of whey protein/gum arabic coacervates. *Biomacromolecules*, 5, 1437–1445.
- Wen, L., & Papadopoulos, K. D. (2001). Effects of Osmotic Pressure on Water Transport in W(1)/O/W(2) Emulsions. *Journal of Colloid and Interface Science*, 235(2), 398–404.
- Wilson, M. A., & Pohorille, A. (1994). Molecular dynamics of a water-lipid bilayer interface. *Journal of the American Chemical Society*, 116(4), 1490–501.
- Winsor, P. A. (1948). Hydrotrophy, Solubilisation and Related Emulsification Processes. Part I. *Transactions of the Faraday Society*, 44, 376–398.
- Yagmur, A., Campo, L. De, & Glatter, O. (2008). Formation and Characterization of Emulsified Microemulsions. In M. Fanun (Ed.), *Microemulsions: Properties and Applications*. Boca Raton: CRC Press.
- Yagmur, A., Campo, L. De, Sagalowicz, L., Leser, M. E., & Glatter, O. (2005). Emulsified Microemulsions and Oil-Containing Liquid Crystalline Phases. *Langmuir*, 21(30), 569–577.
- Yagmur, A., Campo, L. De, Sagalowicz, L., Leser, M. E., & Glatter, O. (2006). Control of the Internal Structure of MLO-Based Isosomes by the Addition of Diglycerol Monooleate and Soybean Phosphatidylcholine, *Langmuir*, 22, 9919–9927.
- Yagmur, A., & Glatter, O. (2009). Characterization and potential applications of nanostructured aqueous dispersions. *Advances in Colloid and Interface Science*, 147-148, 333–342.
- Yagmur, A., Rappolt, M., Østergaard, J., Larsen, C., & Larsen, S. W. (2012). Characterization of Bupivacaine-Loaded Formulations Based on Liquid Crystalline phases and Microemulsions : The Effect of Lipid Composition. *Langmuir*, 28, 2881-2889
- Zhang, H., Feng, F., Li, J., Zhan, X., Wei, H., Li, H., & Wang, H. (2008). Formulation of food-grade microemulsions with glycerol monolaurate : Effects of short-chain alcohols , polyols , salts and nonionic surfactants, 613–619.